

UNIVERSITY OF SURREY

FACULTY OF ENGINEERING AND PHYSICAL
SCIENCES

SUBMITTED FOR THE DEGREE OF MASTER OF
PHYSICS

**Gamma ray and Neutron Pulse
Shape Discrimination in ^6Li
Doped Scintillators**

Author:
Christopher PAYNE

Supervisor:
Dr. Paul SELLIN

February 6, 2012

Abstract

The neutron is a subatomic Hadron of no net charge and a similar mass to that of a proton. There is no direct way of measuring the presence or energy of a neutron, as when looking for a neutron, current radiation detection equipment can only see charged particles created in a reaction, which has had a neutron involved as a reactant. With the advancement of inorganic and organic scintillating materials, specially designed to be used for radiation detection, it has become easier to detect these charged particles. With this comes the need for more advanced pulse processing, in order to clearly distinguish between electrical signals created in a detector, that have been created by neutrons and those that have been created by other sources of radiation or electronic noise. This document focuses on the work done with a set of specially designed scintillator panels, comprised of two types of scintillating material and the digital pulse processing performed on them, in order to distinguish between gamma and neutron pulses within a detector. One of the materials is a plastic scintillator sensitive to gamma radiation whilst the other is a Zn/S layer doped with ^6Li , which is sensitive to neutrons. Up until now no one has successfully been able to separate pulses in one material relating to gammas and neutrons, this work should help towards changing this.

Contents

1	Introduction	4
2	Theory	11
2.1	Gamma and Neutron Radiation Definitions	11
2.1.1	Gamma Radiation	11
2.1.2	Neutrons	12
2.1.3	Thermal Neutrons	13
2.1.4	Fast Neutrons	13
2.2	Gamma Ray Interactions and Neutron Interactions	13
2.2.1	Gamma Ray Interactions	13
2.2.2	Compton Scattering	14
2.2.3	Photoelectric absorption	17
2.2.4	Pair Production	17
2.2.5	Neutron Interactions	18
2.3	Neutron Li^6 Interaction and Reaction Cross Section	20
2.3.1	Reaction Cross Section	20
2.3.2	Neutron Li^6 Interaction	21
2.4	Scintillation Detector Basics	22
2.4.1	Luminescence	22
2.4.2	Molecular Fluorescence Spectroscopy	23
2.4.3	Scintillator Materials	23
2.5	Organic and Inorganic Scintillator Properties	25
2.5.1	Organic Scintillators	25
2.5.2	Organic Plastic Scintillators	27
2.5.3	Light Output	27

2.5.4	Time Response	28
2.5.5	Inorganic Scintillators	30
2.6	Spectroscopy	32
2.7	Pulse Processing Techniques	33
2.7.1	Pulses	33
2.7.2	Analogue Pulse Processing	34
2.7.3	Digital Pulse Processing	35
2.7.4	Comparison of Analogue to Digital Pulse Processing	35
3	Experimental Procedure and Detector Design	38
3.1	Detector Design and The Pixie4 System	38
3.1.1	Schematic	38
3.1.2	Zinc Sulfide as an Inorganic Scintillator	39
3.1.3	AmBe Neutron Source	40
3.1.4	Pixie 4 System	42
3.2	Experimental Procedure	44
4	Gamma Work	48
4.1	Detector Resolution Work	48
4.1.1	Detector Resolution	48
4.1.2	Results	49
4.2	Collimated Cs Source Work	51
4.2.1	Collimated Cs Source	51
4.2.2	Results	52
4.3	Gamma Work Discussion	55
5	Neutron Work	57
5.1	Oscilloscope Trace Work	57
5.1.1	Oscilloscope Traces	57
5.1.2	Oscilloscope Results	58
5.2	Rise Time Measurement and Zn/s Gamma Sensitivity	62
5.2.1	Rise Times	62
5.2.2	Ratio Results	69
5.3	Pulse Shape Discrimination	71
5.3.1	Conditions used for separation	71

6	Conclusions	75
7	Acknowledgments	77

Chapter 1

Introduction

The Discovery of Gamma and Neutron Radiation

The scientific community has been aware of radiation since the start of the 20th century, in 1900 French physicist Paul Villard, discovered gamma radiation whilst studying a piece of Radium but was not named so until 1903 by Ernest Rutherford. 17 years later in 1920, Rutherford, proposed the existence of an uncharged particle which would be found inside the nucleus of an atom, to better explain the difference that was found between the atomic number and atomic mass of elements. This theory was not popular as the accepted opinion at the time was that a nucleus was only made up of protons and electrons. In 1930 Viktor Ambartsumian and Dmitri Ivanenko, two Russian physicists proved that the nucleus could not be made up of protons and electrons, but rather of protons and some other neutral particle.

During the year of 1931, an experiment was done by physicists Walther Bothe and Herbert Becker which produced a highly penetrative type of radiation that was thought to be just another type of gamma ray radiation. The results from this experiment were not clear or easy to interpret as such there was no reason to believe this radiation was anything other than gamma. However in 1932 Parisian scientists, Irene Joliot-Curie and Frederic Joliot-Curie showed that if this radiation was incident on the substance paraffin, the paraffin would eject protons of very high energy. Paraffin is a hydrogen

containing compound, if this new radiation was indeed gamma based, this reaction should not occur thus suggesting that this highly penetrative radiation was not another form of gamma radiation, as previously thought.

It wasn't until 1932 that Rutherford's theory was finally proven by James Chadwick. Whilst working at the University of Cambridge, Chadwick proved that the gamma explanation for this radiation was not correct and instead proved that the nucleus must be made up of a combination of protons and another uncharged particle that had a similar but slightly different mass to that of the proton. He called this new particle, the neutron. The neutron is currently a hot topic for study in the field of radiation detection as it gives further insights to the make up of atoms [1].

Scintillator Materials and Digital Pulse Processing

In recent years the quality of scintillator materials and the ability to process the electrical pulses produced in them have increased and lead to better quality of energy spectra. The combination of the two could lead to devices that are better at detecting radiation which is good for a number of reasons, one such reason in scanning vehicles at army checkpoints in order to locate hazardous materials.

Security Applications

Rapiscan is primarily a radiation detection company who since 1993 have installed over 70,000 products in over 100 countries. Their products range from simple baggage and parcel inspection systems up to equipment specially designed to detect explosive devices and nuclear material. Their systems are in use in airports, government buildings, correctional facilities and even sea ports. Rapiscan have developed a type of scintillation panel which consists of one scintillation panel made of Zn/S doped with ^6Li , sandwiched between two plastic scintillation detectors.

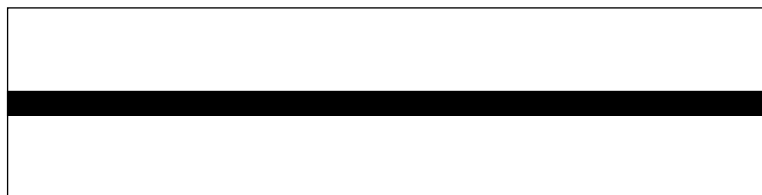


Figure 1.1: Simple RadNuke Schematic, the black section represents the Zn/s layer

The overall design should allow for the detection of gamma rays and thermal neutrons. The plastic scintillators will pick up gamma rays whilst at the same time moderating fast neutrons to slow neutrons so the ${}^6\text{Li}$ panel can interact with them and detect the charged particles created. It is the goal of Rapiscan to develop a detector system that uses digital pulse processing to analyse an object that is placed in front of one of these panels. In the end it should not only be able to tell if radiation is present or not, but from the spectrum obtained it should also be able to identify the source. This work documents the tests done on a set of similar panels using a Varsity of gamma sources and an Am Be neutron source. It also details the digital pulse processing techniques used in order to analyse the data acquired.

The main use for these types of panels is in security applications. Rapiscan have several types of detector systems that are designed to scan vehicles at army checkpoints and smaller ones that are designed to scan baggage. The aim of these systems is to detect either harmful substances or items that could be used as weapons. As this is such an important job these detector systems are all ways being worked on and improved. When no more improvement can be done on the current existing panels, new ones are designed to compensate.

When detecting neutrons, it is the charged particles created in a reaction that one looks for as opposed to the neutron itself as this is a lot easier to do. In the ${}^6\text{Li}$ neutron interaction, two charged particles, an Alpha particle and a Triton are produced with a respective Q value of 4.78 MeV. The reasons for including the gamma detecting panels are two fold, the first is that gamma

ray spectroscopy is a handy tool when it comes to identifying radioactive nuclei and the second is for a use of application reason. The probability that an interaction occurs between two particles can be expressed in terms of a reaction cross section, the higher the cross section of a material the more likely an incoming particle is to hit a particle of that material and interact. In the case where neutrons are the incoming particle, the cross section for ${}^6\text{Li}$ (see figure 1.3) remains small until the energy of the neutrons decrease to an energy of roughly 0.025 eV corresponding to slow neutrons [2]. Fast neutrons can still be detected and this is achieved through neutron moderation which takes place inside the plastic scintillation panels through processes such as scattering (see figure 1.4) to lower their energies.



Figure 1.2: Picture of the Rad-Nuke Vehicle scanning Detector System

The Rad-Nuke portal consists of a set of seven detectors as described before all running in unison. As there is more than one detector, measures must be taken so that the output viewed from one detector is the same as viewed from all others, one thing to think about in this respect is the voltage supply that is fed to each detector. It is this system that is looking to be improved,

the panels used for these experiments consist of just one gamma sensitive panel and the Zn/S sheet however as the materials are the same anything that is found using these panels, will be valid for the same detectors that make up the Rapiscan Rad-Nuke portal. The panels are arranged in an arc which the vehicle must drive through (see figure 1.2).

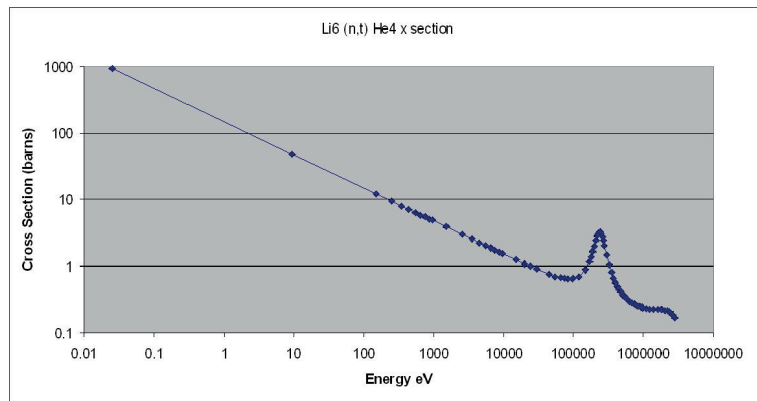


Figure 1.3: The reaction Cross Section for Li^6 [16]

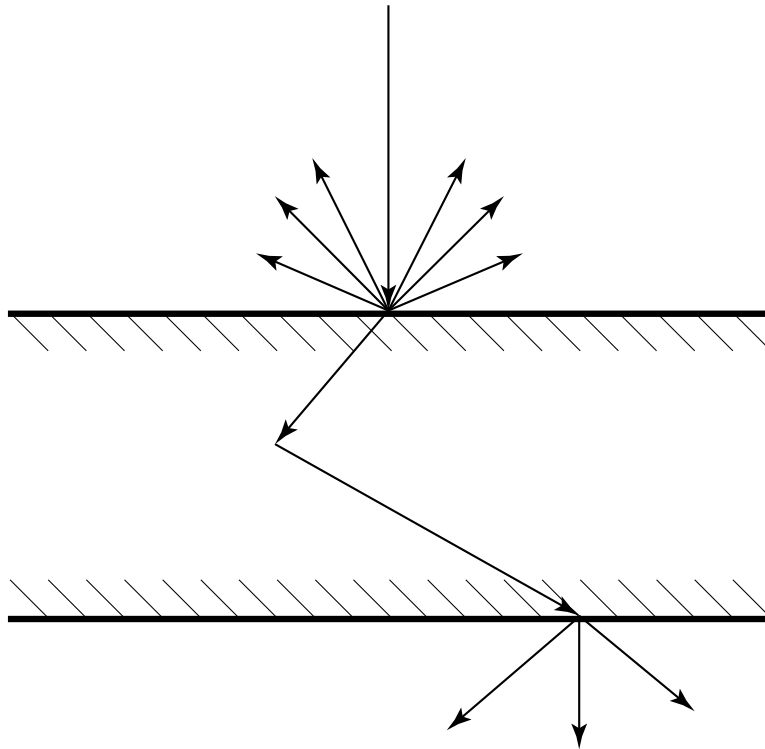


Figure 1.4: Scattering of Neutrons in a Moderator

The methods for detecting gamma radiation and slow neutron radiation differ when using scintillation detectors, as the mechanism required for gamma detection, requires the incident gamma rays to have energies of at least a few eV to work. Slow neutrons are defined as having energies of anything below and up to 0.5 eV which is known as the Cadmium cut off point, this therefore means that slow neutrons have too small of an energy to use the same detection methods as what is used when looking at gamma radiation.

A detector design used to successfully measure both types of radiation is to join together two different scintillating materials, one of which is gamma sensitive, (In this case the plastic scintillator) and the other which is sensitive to slow neutrons (the Zn/S sheet). Both materials are then joined to the same photomultiplier tube which takes the light pulses being created from both scintillators and converts them into electrical signals.

The one problem that arises from this method is that the form that these electrical pulses due to gamma and neutron radiation take, do not relate to each other in anyway apart from the fact that they are both representative of the initial incident radiation that created them. This means that any spectrum produced by simply measuring the amplitude of these pulses and placing them on a typical counts Vs energy graph, will produce a spectrum that has both gamma and slow neutron events but appearing in wrong channels. A Pulse of height x produced in the Zn/s layer will not have the same energy as a Pulse of the same height produce in the Plastic layer, due to reasons such as not being created by the same mechanism and being created in different materials. A simple computer program will not know this so it will place both events in the same channel. The main goal of this project is therefore to design a way to distinguish between gamma and neutron pulses.

Using analogue methods to form the pulses this distinguishing can not be done, however by using more advanced digital pulse processing techniques, this can be done. By looking at the different forms the pulses take in the system, such as different widths and amplitudes, one can tell pulses apart, this is known as pulse shape discrimination. It is the aim of this experiment to see if it is possible to tell the difference between the two types of pulse and apply different energy calibrations to them resulting in a complete spectrum that can be obtained with only one set of detector readings. The main difference that this method will be concerned with, is measuring the different rise times of the two pulses as theory would suggest the pulses created by the thermal neutrons, should have a noticeably longer rise time. The digital system will allow this difference to be detected.

Chapter 2

Theory

2.1 Gamma and Neutron Radiation Definitions

2.1.1 Gamma Radiation

When a heavy nucleus undergoes either alpha or beta decay, the daughter nucleus is often left in a higher, excited energy state. If this state is such that the difference between the current energy level and the ground state is less than the energy needed for fission, the daughter nucleus will de-excite by emitting a high energy photon [1]. Gamma rays form when a nucleus drops from an excited state back into a lower state creating light (Gamma Ray Photon), this light can be absorbed by certain types of radiation detection equipment to measure and record the radioactive events. X-rays have similar wavelengths and energies to gamma rays however they are emitted by electrons outside of the nucleus.

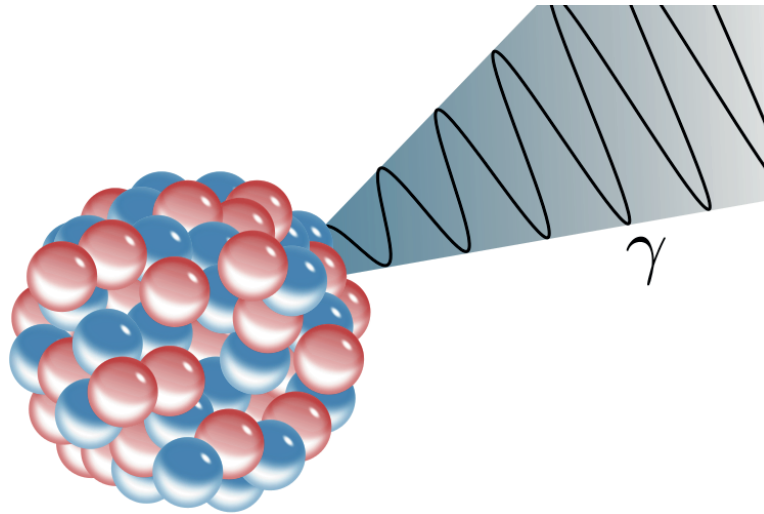


Figure 2.1: A nucleus decaying by emission of a gamma ray, Protons are red and neutrons are blue [3]

2.1.2 Neutrons

The neutron is a subatomic Hadron of no net charge and a similar mass to that of a proton, in general all nuclei of atoms apart from hydrogen consist of a combination of neutrons and protons. Neutrons are generally detected by looking for the energetic particles such as alpha particles and protons that are created in nuclear reactions where a neutron has been the catalyst. The majority of neutron detectors are comprised of a target material that is sensitive to neutrons (such as Li), coupled to a standard radiation detector such as a scintillation detector. Neutrons that are not bound in an atom are unstable and can undergo beta decay, usually in experiments it is these free neutrons that are used. The cross section for neutron interactions in most materials is dependent on the energy of the neutron with lower energies having a better chance to interact. Because of this different methods are used to detect different types of Neutrons which fall into two categories known as thermal and fast neutrons. [4]

2.1.3 Thermal Neutrons

Neutrons that have energy less than 0.5 eV are classed as slow neutrons, it is these neutrons that are found in modern day nuclear reactors and it is the purpose of most detectors in this field to measure the neutron flux. The neutrons having such a low energy cannot be detected by methods such as proton recoil however because their energies are so low, the reaction cross section for certain materials becomes large enough for a reaction to occur more frequently. This leads to the admittance of charged particles that can be measured with the use of standard radiation detectors.

2.1.4 Fast Neutrons

Fast neutrons are classed as high energy neutrons and as such the methods used for detecting them are not the same as for slow neutrons, as the reaction cross section is now too small to acquire any good data. Instead a method known as fast neutron scattering is used, this is where the fast neutron scatters lighter nuclei that can be detected. The neutron imparts most (if not all) of its energy on the lighter nuclei, the recoil nuclei that result from elastic scattering from ordinary hydrogen are called recoil protons and it is these that a lot of detectors are based on.

2.2 Gamma Ray Interactions and Neutron Interactions

2.2.1 Gamma Ray Interactions

Although there are many known ways that gamma rays can interact with matter, there are only three main ways that they do:

- Compton Scattering
- Pair Production
- Photoelectric Absorption

All these processes work in similar ways in that the complete or partial transfer of the energy associated with the gamma ray photon is transferred to an electron within the target material. This sudden transfer of energy is in direct contrast to charged particles that transfer their energy over a series of collisions with a multitude of atoms within a material. [5]

2.2.2 Compton Scattering

In low Z materials such as liquid scintillators or certain types of plastic scintillators, gamma rays interact by Compton scattering [6], and so the general energy spectrum consists of a Compton continuum and edge, but no photo peak. In a scattering event, a photon collides with an electron within the target material depositing part or all of its energy to the electron before moving off at a new angle. The electron absorbs the energy lost by the photon and recoils with a kinetic energy E_e :

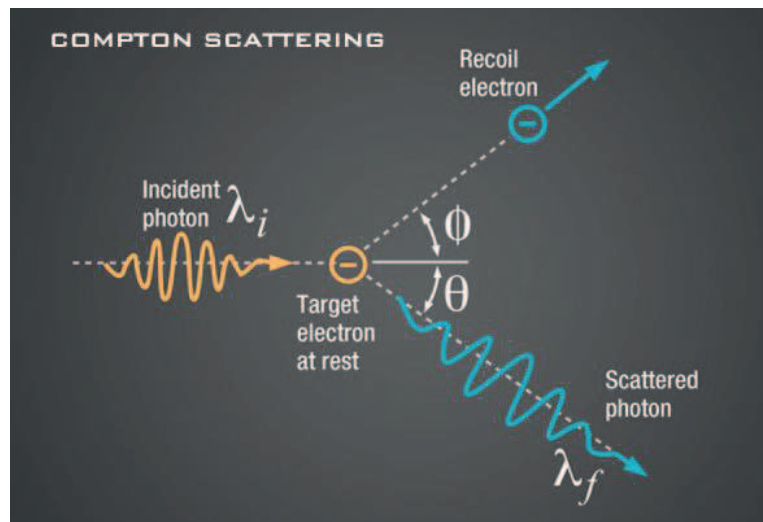


Figure 2.2: A photon of wavelength λ_i comes in from the left, collides with an electron at rest, and a new photon of wavelength λ_f emerges at an angle θ [7]

The conservation of energy means that the energy of the incoming photon

E_p added to the energy of the electron E_e summed is equal to that of the two after collision such that:

$$E_e + E_p = E'_e + E'_p \quad (2.1)$$

By taking into account that photons have momentum and that the energy of a photon is given by

$$E = h\nu \quad (2.2)$$

where h is Planck's constant and ν is the frequency of the wave, one can derive an equation for the change in energy or wavelength that the incident photon has after the collision with the electron. If done correctly the following formula is found.

$$\lambda_f - \lambda_i = \frac{h}{M_e c} (1 - \cos(\theta)) \quad (2.3)$$

where

λ_f is the wavelength of the scattered photon,

λ_i is the initial wavelength,

h is Planck's constant,

M_e is the rest mass of the electron,

c is the speed of light

θ is the scattering angle.

There are two extreme cases of scattering which make up the lower and higher ends of the Compton continuum.

1. Small angle scattering or grazing angle when $\theta = 0$, $\cos(\theta) = 1$. In this circumstance E'_p is almost the same as E_p and so $E'_e = 0$. The recoiling electron has basically no energy and the recoiling photon is scattered at a minimal angle resulting in very little energy loss.

2. A head on collision where $\theta = \pi$. In this circumstance the photon is backscattered along the same direction that it was incident on the electron on. The electron itself recoils along the direction of incidence. In this case the recoil electron energy is given by.

$$E_{\text{MAX}} = E_p \frac{\frac{2E_p}{M_e c^2}}{1 + \frac{2E_p}{M_e c^2}} \quad (2.4)$$

This represents the maximum detectable energy for this mechanism of detection and corresponds to the Compton edge part of the spectrum. As the energy the detector can detect is then within a range of many possible energies, a spectrum forms with a characteristic known as a Compton continuum, the following is an example of this (with a photo peak). The photo peak is not always present but if the process that has occurred is Compton Scattering, the continuum will be.

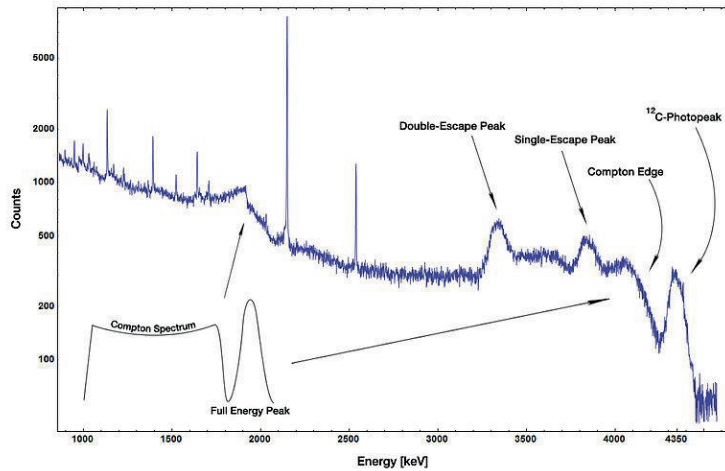


Figure 2.3: Example of Am-Be gamma spectrum with Ideal Compton Continuum [8]

2.2.3 Photoelectric absorption

In the photo electric effect, an incident photon undergoes a reaction with a target atom in such a way that the incident photon disappears completely. An atom will absorb the incident photon and eject a new photo electron from an electron shell, in the case were the incident photon is a gamma ray photon, this will most likely be from the most tightly bound K shell. As the mechanism for this reaction requires the whole atom, it can not take place with a free electron. The photo electron that is created has an energy given by

$$E_e = h\nu - E_b \quad (2.5)$$

Where E_b represents the binding energy of the photo electron from it's original shell. This ejection of a photo electron creates a vacancy in the shell it came from which can be filled by a free electron. This can come from either outside or inside the atom creating a characteristic X-ray, as such the above process can be repeated if the atom then absorbs this X-Ray.

This mode of interaction is the most common for gamma rays of low energy, especially if the target material is a high Z material, as such detectors designed to measure only gamma events, are often made of high Z materials such as Germanium.

2.2.4 Pair Production

If a gamma ray has more than twice the energy of the rest mass energy of an electron, the process of pair production is energetically possible but not necessarily dominant, it does not become so until the gamma rays reach MeV of energy. This reaction takes place within the Coulomb field of a nucleus, as such it can not happen without the presence of an atom. In this reaction the gamma ray photon disappears completely, like in the photoelectric absorption mechanism however this time an electron-positron pair are made. Any energy above 1.02 MeV that the incident photon had is

transferred to kinetic energy between the electron and positron.

Once the positron slows down enough within the material it will annihilate creating two annihilation photons which are both measured in detectors. In a low Z material, the photoelectric cross section is too low for a photo peak to emerge, therefore the only information you can get from a gamma ray interaction is the spread of energy that the gamma ray electrons can take via the most dominant gamma ray interaction, in this case the Compton scattering events.

2.2.5 Neutron Interactions

As with gamma rays, neutrons carry no net charge so they do not interact with matter via the coulomb force which is the dominant means of interaction for charged particles and electrons. However neutrons are also more penetrative than gamma rays and can pass through many cm of materials without undergoing any sort of interaction, this means that they are not seen by common sized gamma detectors [4].

For this reason when trying to detect neutrons it is the charged particles created in a reaction where a neutron has been one of the reactants that a detector looks for. When a neutron does interact, it is with the nucleus of an atom and itself will either disappear completely or have its energy and direction of travel changed severely. Often the created radiation takes the form of heavy charged particles emanating either from the nucleus of the target material itself or a neutron induced nuclear reaction.

Slow neutrons tend to interact with a target in one of two ways, the first is through elastic scattering whilst the second is by neutron-induced events within the target material. Because of the relatively small amount of kinetic energy a thermal neutron has, hardly any energy can be transferred to the nucleus of an atom in elastic scattering, this fact means slow neutron detectors are not designed to detect neutrons this way but rather in

the more probable case of interaction, were a neutron reacts with a target nucleus and creates a set of heavy charged particles that can themselves be seen. The types of favoured reactions that can occur are (n,a), (n,p) and (n,fission) as charged particles are created however another type of reaction can occur using foil targets however the reaction creates a second type of radiation often gamma, making this reaction great for neutron shielding but not necessarily for neutron detection.

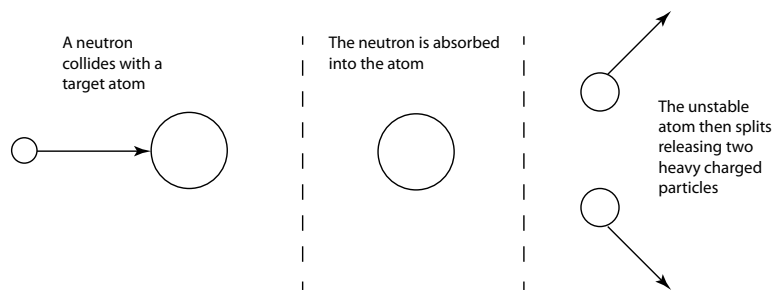


Figure 2.4: Diagram of Neutron-Induced Events

Fast neutrons with higher energies, must be detected in different ways as the probability for neutron-induced events drops drastically with the increase of energy. The main reaction now becomes inelastic scattering, where the created product is a recoil nucleus that if given enough energy will de-excite via the emission of a gamma ray. A neutron will transfer most of its energy to a target of similar mass making materials made of hydrogen the best type for detectors based on this reaction, subsequently, heavier nuclei do not perform as well. In this sense the material is acting as a moderator and as each collision takes a portion of the neutrons energy, hydrogen is considered the best as it can take all of the energy in one collision.

2.3 Neutron Li^6 Interaction and Reaction Cross Section

2.3.1 Reaction Cross Section

The probability of an interaction occurring between some sort of incident radiation and a target atom, electron or nucleus can be expressed in terms of a reaction cross section. An incident radiation will have a flux of I_o , consider this beam arriving at an absorber at right angles to it. The absorber itself has element thickness dx and surface area Q . The transmitted flux, (or the amount of radiation per unit area per unit time) that was not absorbed, can then be expressed as $I_x = I_o + dI$, where dI is the change in Flux. The Volume of the element can be expressed as $Q \cdot dx$, if the materials atomic density is N atoms per unit volume, the element then contains $NQ \cdot dx$ atoms. Each atom has a removal cross-section J , nuclear overlap is negligible, we have a total target area of removable as $NQJ \cdot dx$. [10]

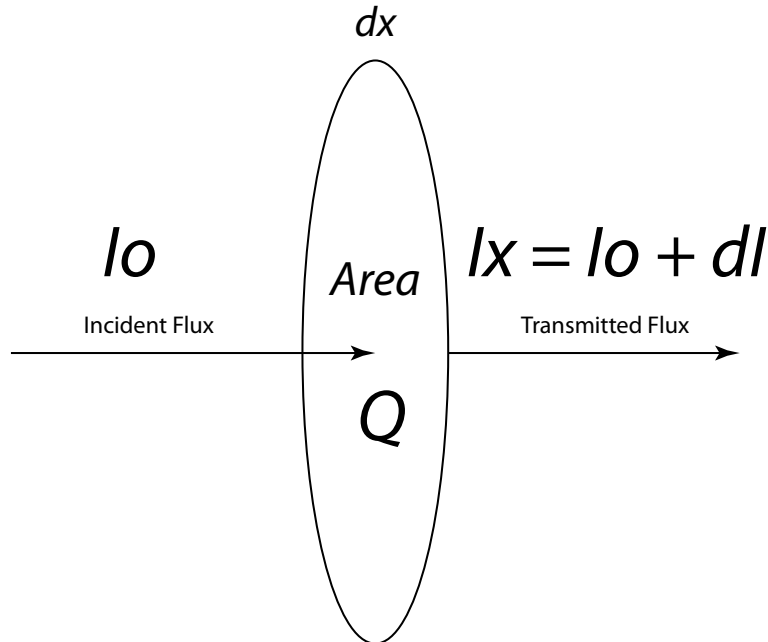


Figure 2.5: Reaction Cross Section Diagram

Working this through to its conclusion results in.

$$I_x = I_o \exp(-\mu x) \quad (2.6)$$

Where μ is the linear attenuation coefficient and is simply given by

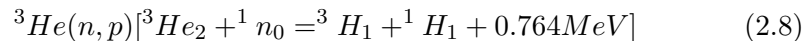
$$\mu = NJ \quad (2.7)$$

This coefficient can be used to work out the mean free path, λ , of the material and is given by $\lambda = \frac{1}{\mu}$ equation 2.6 can then also be written as $I_x = I_o \exp\left(-\frac{x}{\lambda}\right)$. $\frac{x}{\lambda}$ is therefore the absorber thickness expressed in an amount of mean free paths. I_x/I_o gives the fractional amount of radiation passing through a material, the fraction absorbed is then simply $1 - I_x/I_o$ which is the intrinsic detection efficiency, for ideal detection, you want this value as close to one as possible. Nuclear cross sections are expressed in Barns where 1 Barn = 10^{-28} m², corresponding to the circular cross sectional area of what ever atom the material is made of.

Particles have a de Broglie Wavelength given as $\lambda = \frac{h}{m_v}$ where m_v is the linear momentum of the particle. The lower the energy therefore the bigger the wavelength, when this wavelength becomes bigger it has more of a chance of interacting as it becomes larger than the nuclear radius of the atom, for neutrons to be detected in this method they need to have low energies, the best results for this are achieved with thermal neutrons.

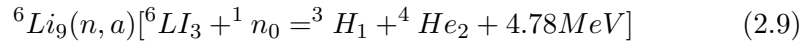
2.3.2 Neutron Li6 Interaction

There are few atoms that make for good neutron detectors where the desired reaction results in the creation of two charged particles, the best atom to use is that of He. The reaction for He is the following [4].



However due to He benefits it has become highly popular and as it is used in many other areas, not just in radiation detection, it is vary costly to

create large detectors from it. An alternate atom to use (and the one this paper focuses on) is Li6. The reaction for a neutron with Li6 is the following.



In this reaction, the neutron is absorbed and creates two charged particles that have similar energies, one is an alpha particle, whilst the other is a Triton. Li is much cheaper than He so could be a viable alternative for large scale neutron detectors if it is proven to be good enough. The reaction cross-section for thermal neutrons, all though not as good for He, is still good as at low energies the cross section increases, a graph of this can be seen in the introduction. This sort of reaction all though possible is highly unlikely to work for fast neutrons, however as neutron energy increases the elastic-cross section for neutrons increases, making detectors that work on the principles of proton recoil are used.

2.4 Scintillation Detector Basics

2.4.1 Luminescence

Luminescence is the term given to the emission of light from a substance. This process occurs when an electron in an excited state, loses energy by emitting a photon and drops back down to the electron ground state. Luminescence can only be described using quantum physics and not in classical terms, as quantum physics states that the possible energy values a system can take, are determined by its internal properties, i.e. it's structure. Often the emitted light will have slightly less energy than that of the difference between the two energy states, this energy however is still characteristic of the material, so a form of luminescent spectroscopy can be done from looking at the emitted light. This is known as the first law of luminescence and was formulated by Stokes in 1852. The law states “The wavelength of luminescence excited by radiation is greater then the wavelength of the exciting radiation.” [11]

Luminescence Spectroscopy is the name given to three related spectroscopic techniques.

- Molecular fluorescence spectroscopy
- Molecular phosphorescence spectroscopy
- Chemical luminescence spectroscopy

2.4.2 Molecular Fluorescence Spectroscopy

Particles have a set of different states known as energy levels. In the case of an electron in an atom, the higher energy states relate to the electron itself having a higher energy. Fluorescence Spectroscopy relates mainly to the vibrational states and the electronic states. Normally a particle will consist of a ground state (minimum energy) and a set of excited electronic states which have vibrational states between them. In practice a particle will be excited from the ground state to an excited state through the absorption of a photon, it will then begin to lose energy through collisions with other particles until it reaches the lowest vibrational level within the current electronic level. At this time to drop back down to a lower excited state, a photon must be emitted. As the particle can drop back down to any of the vibrational states in the lower level a set of different photons with different wavelengths can be emitted. It is these differences that are measured in order to determine the structure of the different vibrational states. In an experiment a single wavelength beam can be used to excite a sample and the fluorescence measured to produce emission spectrum. This spectrum can tell you what material the sample is if you do not know.

2.4.3 Scintillator Materials

Scintillation is the term used when specifically talking about the luminescence that is produced when ionising radiation is incident on a scintillation material.

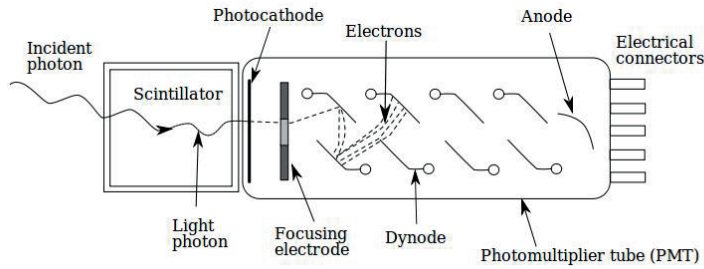


Figure 2.6: A basic Scintillator Detector Design [12]

A scintillator is a material that when struck by a form of ionising radiation, absorbs the energy from the particle and then readmits it as light, this process is known as luminescence. This property can be used in radiation detection, when a scintillator is coupled to a photomultiplier tube a scintillator detector is made. The light emitted from the material is again absorbed by the PMT and emitted as electrons via the photoelectric effect. The multiplication of these photoelectrons can then be turned into an electrical signal that can be analysed resulting in the formation of data corresponding to the initial energy of the photon that is emitted from the material.

Figure 2.6 shows a schematic of a scintillator detector, incident photons strike the photocathode material and create electrons via the photoelectric effect, these electrons are then accelerated towards the first dynode which is held at some positive voltage, increasing in energy as they travel. Once they strike the dynode itself, more low energy electrons are created which are once again accelerated towards the second dynode which is held at a higher voltage than the first. This process is repeated until the electrons reach the anode where the accumulation of charge is converted into a measurable electrical signal.

This signal can be amplified by changing the voltage that is supplied to the PMT by increasing the voltage you increase the signal but at the cost of a lower signal to noise ratio.

The main properties an ideal scintillation material should have are the following.

1. It should convert the energy of the incident charged particles into detectable light with a high efficiency.
2. This conversion needs to be linear, the light intensity created should be proportional to the initial energy over a wide range.
3. The material should be transparent to wavelengths of its own emission as to avoid re absorbing.
4. The decay time of the created light should be short so fast pulses can be created.
5. The material itself should be good quality and easily manufacturable.
6. The index of refraction of the material should be close as possible to that of glass to allow the best coupling to a PMT.

No one material can fit all 6 of these points, so often a compromise must be made between them.

2.5 Organic and Inorganic Scintillator Properties

2.5.1 Organic Scintillators

The process of fluorescence in organics comes from the transition in energy levels of a single molecule as such the physical state of the system plays no part in the process [4]. This is in direct contrast with inorganic scintillators that require a regular crystalline lattice as a base to achieve the scintillation process. The energy levels of an organic molecule are represented by a system known as the pi-electron structure. The most stable state of a molecule is known as the ground state and is the lowest energy a molecule can have. It is represented by the notation S_{00} . The first 0 in this notation relates to

the singlet state which the molecule is in (Spin 0 for this case). Each singlet state can be divided into a set of vibrational states that have a separation of roughly 0.15 eV. S_{00} therefore relates to a spin of 0 with the lowest vibrational state, S_{01} relates to the next highest energetic state which is one vibrational state higher than the ground state. S_{02} is one more vibrational state than S_{01} and so on. A molecule can be excited into a higher state by the absorption of kinetic energy from a charged particle, however if it is excited into one of the vibrational states within S_0 it will de-excite through internal mechanisms that release no radiation. This structure can be seen in figure 2.7 [4].

For light to be emitted, the transition must be between singlet states e.g. S_1 to S_0 , typical energy gaps between adjacent singlet states are 3 to 4 eV. Due to the fact that the energy spacing between vibrational states is large when compared to the average thermal energies a molecule is in (0.025 eV) a molecule in a standard situation will be found in the ground state and needs something external to excite it into a higher one. The main source of light (fluorescence) that detectors measure, comes from the transition in energy from S_{10} to one of the Vibrational states of S_0 . The time in which it takes a newly excited state to decay back down, in an organic material is short, usually a few nanoseconds making the prompt scintillation component relatively fast.

Figure 2.7 helps to explain why organic materials are useful as the energy of the emitted light, tends to be less than what it takes to excite S_0 to S_1 meaning it fully fills rule 3 of what makes a good scintillator. Some radiationless de-excitations can still occur from the S_1 to S_0 state and these all fall under the term quenching but this is not normally an issue.

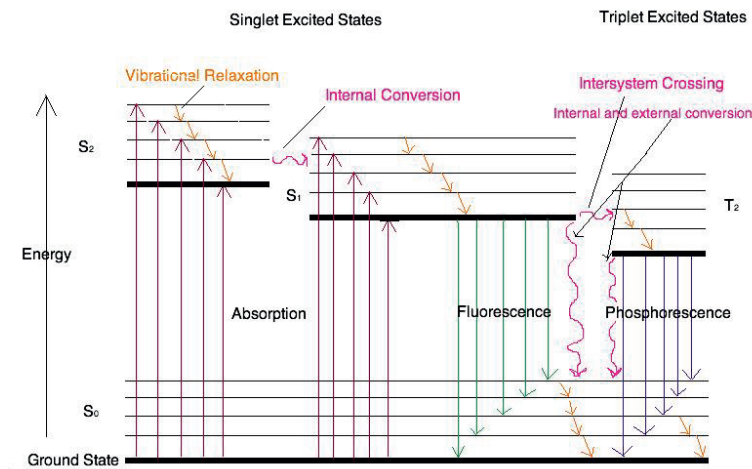


Figure 2.7: Energy States within a Molecule [13]

2.5.2 Organic Plastic Scintillators

A solid plastic scintillator can be created by dissolving an organic scintillator in a solvent and then polymerized. Plastic scintillators are often the cheapest solution to simple gamma ray detection. This is because they are cheap and often the only solution when it comes to making large scale detectors designed to scan large areas as costs would rise significantly if the detector was made from anything else. There are a few drawbacks however when creating such large plastic scintillators, one is that the case of self absorbing its own light may no longer be negligible and the second is the light intensity may change significantly as it moves through the plastic due to attenuation.

2.5.3 Light Output

Only a portion of the kinetic energy lost by a charged particle in a scintillator is converted into light energy. The amount of energy transferred relates to both the type of incident particle and its energy. For the case of electrons, the response to energies above 125 KeV is linear, the response for charged particles such as alpha particles, is always less for equivalent energies, see figure 2.8. As initial energies increase, the response of the two begin to come together however there is still a difference, at low energies this difference is

as much as 10 times bigger. It is important to remember this fact when using an organic material to detect both types of radiation as the light pulses produced in the material will be different although they could be representative of the same energies. It is for this reason that more complicated pulse processing is needed to properly distinguish between them.

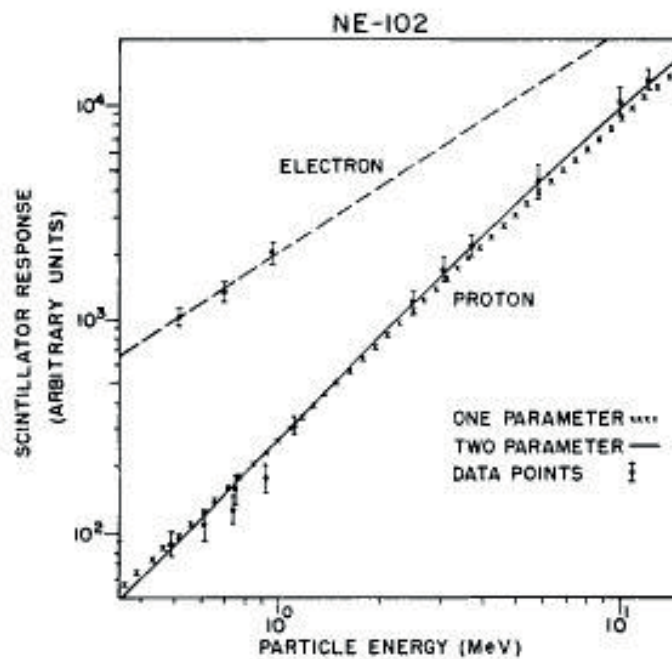


Figure 2.8: Light Yield Comparisons, alpha particles fall roughly on the same line as the protons do [14]

2.5.4 Time Response

In organics luminescent states are formed instantly and only prompt fluorescence is present, therefore the form that a typical light pulse takes in an organic material can be thought of as having a sharp rise time, followed by an exponential decay. The following is a table of common organic scintillator materials and their associated properties.

Table 8.1 Properties of Some Commercially Available Organic Scintillators

NE	Eljen	St. Gobain	Light Output %Anthracene*	Wavelength of Max Emission (nm)	Decay Constant (ns)	Attenuation Length (cm)	Refractive Index	H/C Ratio	Density	Loading Element % by weight or dist. feature	Softening or Flash Point (°C)	Uses
	Crystal											
	Anthracene		100	447	30		1.62	0.715	1.25		217	
	Stilbene		50	410	4.5		1.626	0.858	1.16		125	
	Plastic											
NE-102A	EJ-212	BC-400	65	423	2.4	250	1.581	1.103	1.032		70	General purpose
NE-104	EJ-204	BC-404	68	408	1.8	160	1.58	1.107	1.032	1.8 ns time constant	70	Fast counting
Phos F	EJ-200	BC-408	64	425	2.1	380	1.58	1.104	1.032		70	TOF counters, large area
NE-110	EJ-208	BC-412	60	434	5.3	400	1.58	1.104	1.032	Longest atin. length	70	General purpose, large area, long strips
		BC-420	64	391	1.5	110	1.58	1.100	1.032	1.5 ns time constant	70	Ultrafast timing, sheet areas
NE-111A	EJ-232	BC-422	55	370	1.4	8	1.58	1.102	1.032	1.4 ns time constant	70	Very fast timing, small sizes
		BC-422Q	11	370	0.7	< 8	1.58	1.102	1.032	Benzophenone, 1%	70	Ultrafast timing, ultrafast counting
NE-103	EJ-260	BC-428	36	480	12.5	150	1.58	1.103	1.032	Green emitter	70	Photodiodes and CCDs; phoswich detectors
NE-108		BC-430	45	580	16.8	NA	1.58	1.108	1.032	Red emitter	70	Silicon photodiodes and red-enhanced PMTs
		BC-436	52	425	2.2	NA	1.61	0.960 D-C	1.130	Deuterium, 13.8%	90	Thin disks
NE-115	EJ-240	BC-444	41	428	285	180	1.58	1.109	1.032		70	Phoswich detectors for <i>dE/dx</i> studies
NE-142	EJ-256	BC-452	32	424	2.1	150	1.58	1.134	1.080	Lead, 5%	60	X-ray dosimetry (< 100 keV)
		BC-454	48	425	2.2	120	1.58	1.169	1.026	Boron, 5%	60	Neutron spectrometry, thermal neutrons
NE-105	EJ-252	BC-470	46	423	2.4	200	1.58	1.098	1.037	Air equivalent	65	Dosimetry
		BC-490	55	425	2.3		1.58	1.107	1.030	Casting resin	70	General purpose
		BC-498	65	423	2.4		1.58	1.103	1.032	Applied like paint	70	β , γ detection
	Liquid											
NE-213	EJ-301	BC-501A	78	425	3.2		1.51	1.212	0.874	Pulse shape discrim.	26	γ > 100 keV, fast n spectroscopy
NE-224	EJ-305	BC-505	80	425	2.5		1.50	1.331	0.877	High light output	47	γ , fast n, large volume
	EJ-309		75	425	3.5		1.57	1.25	0.964	High flash point	144	pulse shape discrimination
NE-226	EJ-313	BC-509	20	425	3.1		1.38	0.8055	1.61	F	10	γ , fast n
	EJ-321H	BC-517H	52	425	2.0		1.89	0.86		Mineral oil-based	81	γ , fast n, cosmic, charged particles
		BC-517P	28	425	2.2			2.05	0.85	Mineral oil-based	115	γ , fast n, cosmic, charged particles
NE-235C	EJ-325	BC-519	60	425	4.0		1.73	0.875		Pulse shape discrim.	74	γ , fast n, n- γ discrimination
NE-323	EJ-331	BC-521	60	425	4.0		1.31	0.89		Gd (to 1%)	44	Neutron spectroscopy, neutrino research
NE-321A	EJ-339	BC-523A	65	425	3.7		1.67	0.93		Enriched ^{10}B	1	Total absorption neutron spectrometry
	EJ-335	BC-525	56	425	3.8		1.57	0.88		Gd (to 1%)	64	Neutron spectrometry, neutrino research
		BC-533	51	425	3.0		1.96	0.8		Low temp operation	65	γ , fast n, cosmic
NE-230		BC-537	61	425	2.8		1.50	.99 (D-C)	0.954	^2H	-11	Fast n, pulse shape discrimination
NE-314A		BC-551	40	425	2.2		1.31	0.902		Pb (5% w/w)	44	γ , X-rays < 200 keV
		BC-553	34	425	3.8		1.47	0.951		Sn (10% w/w)	42	γ , X-rays

*NaI(Tl) is 230% on this scale

Figure 2.9: Organic Scintillator Materials [4]

2.5.5 Inorganic Scintillators

The structure of the crystalline lattice in inorganic scintillators, is what determines the scintillation mechanism. In a crystal, electrons can only occupy discrete energy levels in the lower energy band (Valance Band) or the upper energy band (Conduction Band). Electrons in the valance band are bound at lattice sites and can not move throughout the crystal, however if the electrons have sufficient energy they can leave the valance band and enter the conduction band leaving a hole behind in the valance band. Whilst in the conduction band the electron is free to move around, any free electron that then comes close to the produced hole can de-excite by emitting a light pulse and be re absorbed into the valance band. There is an energy area between the two bands known as the forbidden band gap were no electrons can ever be found meaning that the light produced can only take discrete energy levels representative of the band gap [4].

To maximise the chance of this process occurring, impurities are often added to the inorganic crystal, these activators create sites within the lattice were the traditional band gap is modified creating sites within the forbidden band gap that electrons can occupy. It is these impurities which determine the structure of any measured energy spectra. Figure 2.10 is a table of some of the more common inorganic scintillator materials along with their properties.

Table 8.3 Properties of Common Inorganic Scintillators

	Specific Gravity	Wavelength of Max. Emission	Refractive Index	Decay Time (μ s)	Abs. Light Yield in Photons/MeV	Relative Pulse Height Using Bialk. PM tube	References
Alkali Halides							
NaI(Tl)	3.67	415	1.85	0.23	38,000	1.00	
CsI(Tl)	4.51	540	1.80	0.68 (64%), 3.34 (36%)	65,000	0.49	85, 105, 106
CsI(Na)	4.51	420	1.84	0.46, 4.18	39,000	1.10	112
LiI(Eu)	4.08	470	1.96	1.4	11,000	0.23	
Other Slow Inorganics							
BGO	7.13	480	2.15	0.30	8200	0.13	
CdWO ₄	7.90	470	2.3	1.1 (40%), 14.5 (60%)	15,000	0.4	119–121
CaWO ₄	6.1	420	1.94	8	15,000		123
SrI ₂ (Eu)	4.6	435		1.2	85,000		125
ZnS(Ag) (polycrystalline)	4.09	450	2.36	0.2		1.3 ^a	
CaF ₂ (Eu)	3.19	435	1.47	0.9	24,000	0.5	
Unactivated Fast Inorganics							
BaF ₂ (fast component)	4.89	220		0.0006	1400	na	133–135
BaF ₂ (slow component)	4.89	310	1.56	0.63	9500	0.2	133–135
CsI (fast component)	4.51	305		0.002 (35%), 0.02 (65%)	2000	0.05	140–142
CsI (slow component)	4.51	450	1.80	multiple, up to several μ s	varies	varies	141, 142
CeF ₃	6.16	310, 340	1.68	0.005, 0.027	4400	0.04 to 0.05	83, 146, 147
Cerium-Activated Fast Inorganics							
GSO	6.71	440	1.85	0.056 (90%), 0.4 (10%)	9000	0.2	156–160
YAP	5.37	370	1.95	0.027	18,000	0.45	85, 165
YAG	4.56	550	1.82	0.088 (72%), 0.302 (28%)	17,000	0.5	85, 167
LSO	7.4	420	1.82	0.047	25,000	0.75	170, 171
YSO	4.54	420		0.070	24,000		152, 153, 155
LuAP	8.4	365	1.94	0.017	17,000	0.3	178, 180, 183
LaCl ₃ (Ce)	3.79	350		0.028	46,000		212
LaBr ₃ (Ce)	5.29	380	2.05–2.10	0.026	63,000		212, 218
Glass Scintillators							
Ce activated Li glass ^b	2.64	400	1.59	0.05 to 0.1	3500	0.09	84, 241
Tb activated glass ^b	3.03	550	1.5	~3000 to 5000	~50,000	na	241
For comparison, a typical organic (plastic) scintillator:							
NE102A	1.03	423	1.58	0.002	10,000	0.25	

^afor alpha particles

^bProperties vary with exact formulation. Also see Table 15.1.

Source: Data primarily from Refs. 81 and 82, except where noted.

Figure 2.10: Inorganic Scintillator Properties [4]

Included in the table is the properties of Zn/S which is the material the second scintillator is made of, the pulses that come from this material have the best pulse amplitude of all of the ones listed and all though blank in this table, it has one of the highest light yields. By just looking at the two tables for organic and inorganic properties, it can be seen that their properties vary by a great amount, for example the decay times in the inorganic materials are a lot smaller then those of the organic ones, coupled in with the light attenuation in the organic material it can be seen that the pulses created will not be the same.

2.6 Spectroscopy

A gamma ray photon carries no net charge and as such does not cause any ionization or excitation within materials that it passes through. This means that for a gamma ray to be detected in something such as a scintillation detector, it must first undergo an interaction that transfers all or part of the photon energy, to an electron within the detection material. The type of reaction involved is a sudden change/transfer in energy as opposed to the slower method of slowing down heavy charged particles through multiple collisions within the target material. Due to the mechanics of these interactions, it is only the newly formed gamma ray electrons that allow one to determine the nature of the incident gamma ray photons as they themselves are not seen by the detector.

The maximum energy one of these electrons can take is equal to the energy that the incident photon had, this does not mean however that the detector will always register this or at all, it all depends on how the detector is made. A good scintillation detector must first do two things, it must be able to react with the incident gamma ray photons, with a high enough probability to create the new gamma ray electrons, a material that is good at this is known as a conversion material. The second function then must be for it to act as a detector for these newly created electrons. This can be done by either having one material to do all of the work, or two joined together that each do one of the two tasks.

FWHM is a number used to express detector resolution. This value is simply the width of a photo peak (given in eV) at half of its amplitude. Detector Resolutions are usually given in terms of gamma ray energies, for example a Sodium Iodide detector could be said to have a resolution of 9 KeV at 611KeV corresponding to a Cs137 gamma ray. This means that if two energies are more than 9 KeV apart around 611 KeV, the detector should be able to tell the two apart and show two separate peaks. Detector resolution can also be expressed as a percentage by taking the FWHM and dividing by the gamma ray energy.

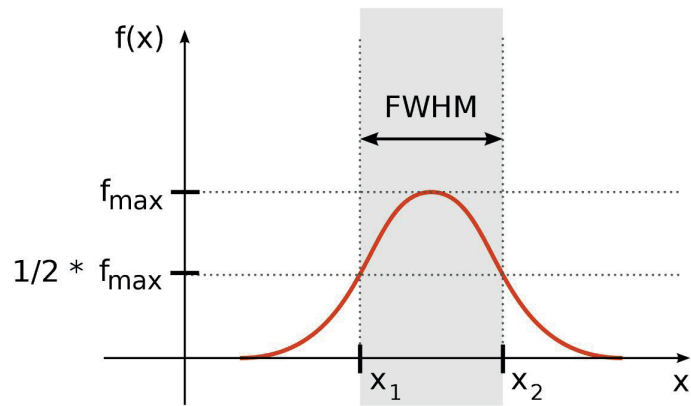


Figure 2.11: Full Width Half Maxima Example

2.7 Pulse Processing Techniques

2.7.1 Pulses

A pulse is the electrical representation of a charge created in a detector when a photon or a particle interacts with the material of a detector. This charge is usually proportional to the initial energy of the photon/particle that was used to create it. Each event counts as one pulse so a series of pulses can be used to measure the count rate of a source, or by measuring the amplitude of the individual pulses, produce an energy spectrum that is representative of the radioactive source. A pulse can be broken down into segments that describe what it looks like.

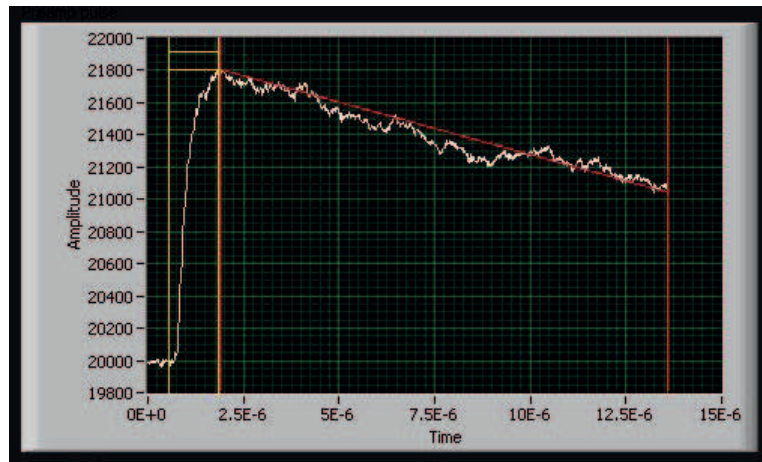


Figure 2.12: Example of a Signal Pulse from a PMT

Above is an example of an electrical pulse that has been recorded using digital pulse processing methods. The amplitude of this pulse (21800 arbitrary units) is what is used to determine the energy of the incident particle that was used to create it. A program will measure the amplitudes of several pulses and place those with higher amplitudes in higher numbered channels than those with lower amplitudes. Users can then set an energy calibration to these channels if required. The section marked in yellow is known as the rise time, this is the time it takes for the electrical signal to reach its maximum amplitude, the red section is known as the decay time.

2.7.2 Analogue Pulse Processing

Analogue pulse processing uses electronic equipment to process electronic signal pulses that arise when a radiation detector is in the presence of a radioactive source. The signal from a pre-amplifier output goes to a shaping amplifier and then on to a multi channel analyser. The shaping amplifier works to shape the input pulse so that an accurate measurement of the pulse height can be measured. Pulse shaping reduces the overall noise of a signal, it works towards reducing pulse pile up and removes the direct current baseline [15].

2.7.3 Digital Pulse Processing

A DPP digitises the signal from a pre-amplifier output, applies digital pulse processing techniques onto the signal which then allows it to accurately measure the amplitude of the signal pulse digitally, this value can then be binned into its histogramming memory so that an energy spectrum can be built. More advanced DPPs can also record the form that each incident pulse takes [15].

Traditional analogue circuitry will not allow you to do any sort of pulse analysis as the pulse shape is not recorded at any point, only the amplitude of the pulse is needed. With the improvement of fast analogue to digital converters however it is now possible to record each individual pulse that is created, this allows you to play back data acquisitions at a later time with certain restrictions added to how the program treats them. These restrictions can be found by first manually analysing the pulses that have been created.

2.7.4 Comparison of Analogue to Digital Pulse Processing

DPPs can be used to replace many of the standard components in an analogue processing system such as the multi channel analyser, any pulse shaping logic devices and many more auxiliary circuitries. They do this by making use of software which in commercial DPPs can be found written into the hardware or by running the digitized signals through software that the user has created in another program.

Figure 2.13 shows a comparison of the components used between a digital and an analogue processing system.

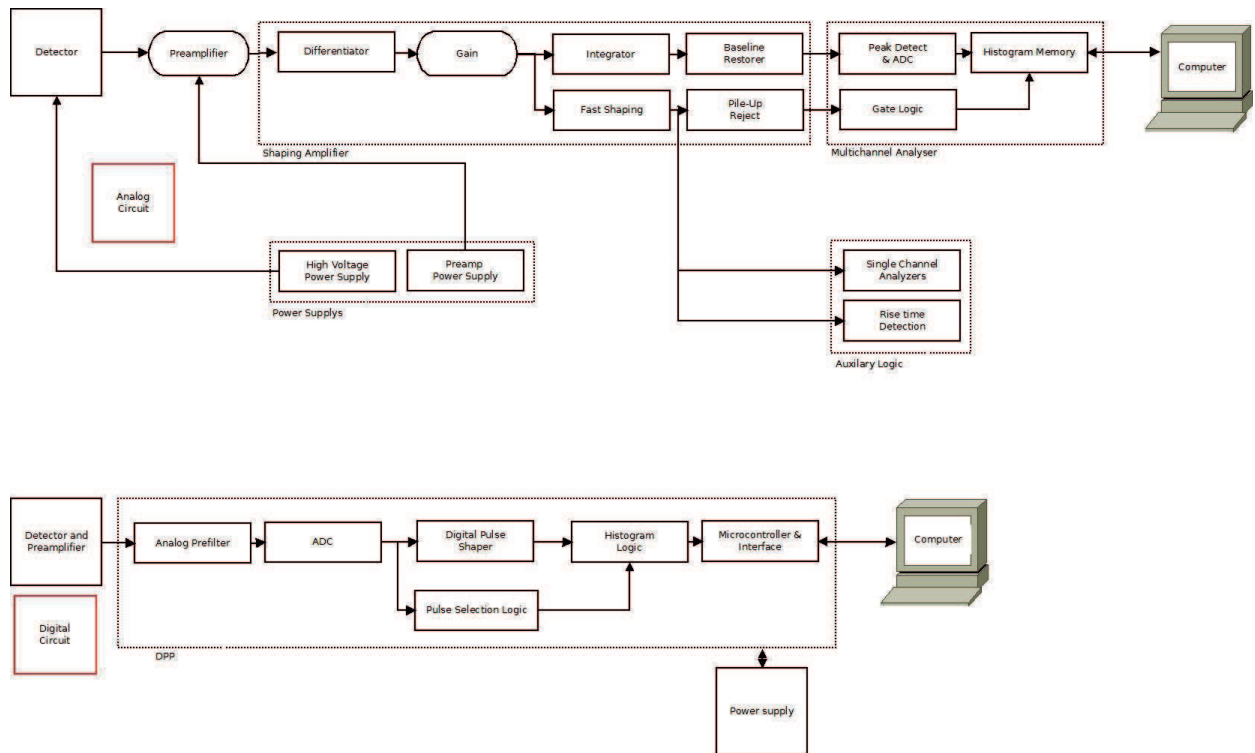


Figure 2.13: Schematic of analogue/digital processing systems

The block diagram for the analogue process shows the basic set-up of any normal processing system. It shows the detector, pre-amplifier, shaping amp, MCA and computer. With this many extra components can be added to further increase the ability to shape the pulses and acquire data. In comparison the block diagram for the digital process shows a lot less components as the analogue to digital conversion takes place sooner than it does in the analogue instrument setup. The conversion occurs straight after the pre-amplifier as opposed to after the shaping amp, this allows all of the pulse shaping and analysis to be done within the DPP itself saving on space and more importantly time.

With traditional circuitry only a finite number of shaping variables can be achieved and this is usually done by turning a dial on the front of the shaping amp to the desired amount. More advanced users can manually replace resistors and capacitors within the circuitry of the amplifier to obtain other

values but this can be delicate and time consuming work. In a DPP all this shaping is done in real time by software so any number of values can be chosen as long as the software permits it, this also allows other shaping techniques that are not possible or easily done using analogue equipment such as trapezoidal shaping.

Chapter 3

Experimental Procedure and Detector Design

3.1 Detector Design and The Pixie4 System

3.1.1 Schematic

The experiments carried out within this paper, have all been conducted using at least one of a set of specially designed scintillation panels which have been built in order to detect and distinguish between incident gamma rays and incident neutron radiation.

The setup consists of a total of 4 panels, the first of these panels is comprised of two separate scintillation materials. One of these materials is a solid plastic scintillator that can detect gamma radiation, whilst the other (which is placed on top of the plastic) is a Zn/S layer doped with Li that can be removed for testing purposes and is designed to detect neutrons. A photo multiplier tube is attached to the plastic scintillator and is the device used to convert any light pulses from the plastic or Zn/S into electrical pulses for measurement.

The surface area for each material measures 50cm by 30cm with the plastic layer having a depth of 1” and the Zn layer a depth of 1mm. The second detector is identical to the first, however the depth of this panel is now 1.5”

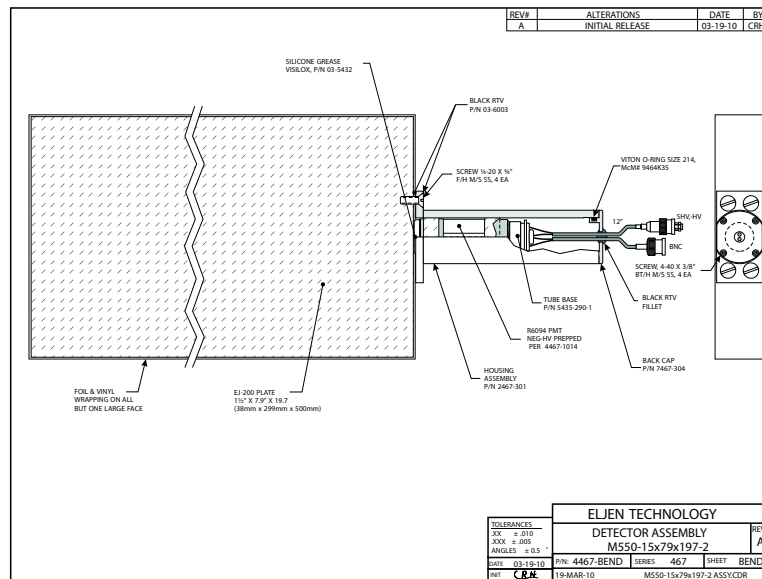


Figure 3.1: Schematic of the Type of Panels used in all experiments written about in this paper.

but apart from this the two are identical. The third and fourth detectors are again identically to the first two having the same depths of 1” and 1.5”. However this time the plastic scintillator has been replaced with an unactivated plastic that can not detect any form of radiation, in theory this then acts purely as a light guide for any light pulses being created in the Zn/S layer due to neutrons.

3.1.2 Zinc Sulfide as an Inorganic Scintillator

Zinc sulfide was one of the earlier materials used as a basis for inorganic scintillators as its high light yield was vary desirable. However as it is only available as a polycrystalline powder, it is limited in that it can only be made into thin screens as too thick and the material would once again break rule 3 of what makes a good scintillator.

The pulses created in these panels come from both the two types of scintillator under different mechanisms (see theory). Theory would suggest that the rise times of the pulses will be different. For gamma rays this time should be

roughly 1 μs where as for the slow neutrons it should roughly be 10 μs . The reason the rise times of the two pulses differ is because the charge recorded by the gamma rays is created when a gamma ray excites an electron to a higher state within the plastic and decays back down to emit light where as the light in the Zn/S layer is created when a slow neutron is absorbed by a Li atom and a alpha and triton particle are created and then again reabsorbed into the Zn/S. Further more this light has to then pass through the plastic Scintillator layer to reach the PMT resulting in a pulse with a longer rise time (see theory for more details).

Without digital pulse processing, pulses with the same amplitude will be binned into the same energy channel in a spectrum, however if they come from different sources they will not be representative of the same energies. By measuring the rise times of the pulses and applying different energy calibrations to the longer rise times than the shorter, this problem could be solved.

3.1.3 AmBe Neutron Source

A standard laboratory source (and the one used for these experiments) of neutrons is the AmBe generator. This comprises a high activity (GBq) ^{241}Am source (a long lived alpha-emitter with $T_{1/2} = 433$ years) that is mixed with beryllium (Be) powder and placed in a sealed can. Neutrons are generated through the ^9Be (alpha) reaction with energies in the range 0-11 MeV. For reference, an 18.5 GBq AmBe source has an output of 10^6 neutrons per second. AmBe sources are typically placed in a water tank such that the fast neutrons are slowed down to thermal energies through multiple scattering with hydrogen in the water molecules. This occurs over a distance of a few cm and generally results in neutron capture through the reaction $1\text{H}(n,\alpha)2\text{H}$ in which deuterium is formed[6].

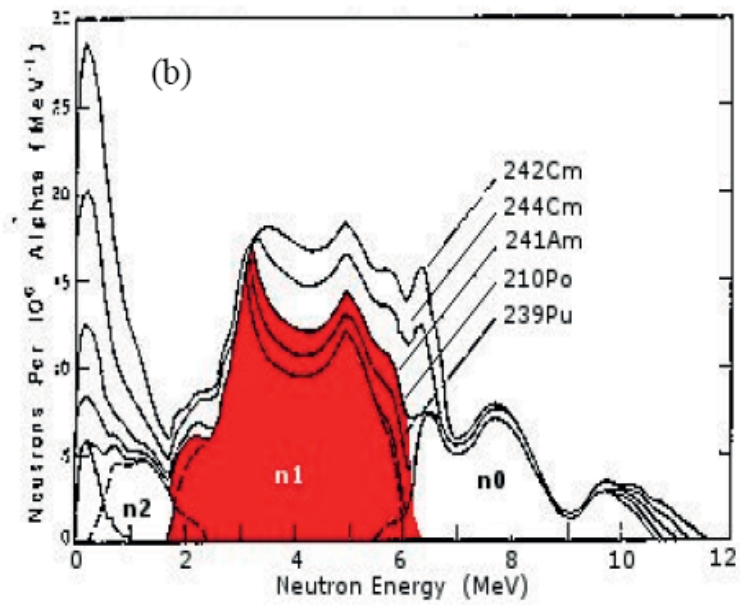


Figure 3.2: Calculated neutron energy spectrum from various actinide-based sources. The red section is the energy spectrum of the neutron source used in these experiments

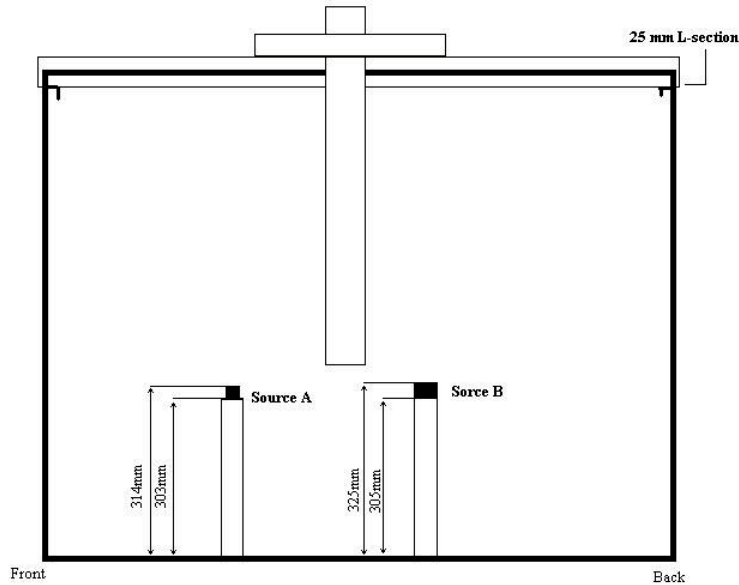


Figure 3.3: [Schematic diagram of the Am-Be (source B) neutron source mounted in the water tank, and the adjustable air pipe.

3.1.4 Pixie 4 System

Because of the complexity of the signal pulses being produced within the PMT from the different light sources, digital pulse processing is needed in order to separate out the pulses relating to gammas and neutrons. To do this the Pixie4 system, a pulse data acquisition system created by the company XIA has been used to record the raw pulse data from the experiments where both gamma and neutrons are present.

“The DGF Pixie4 is a 4-channel all-digital waveform acquisition and spectrometer card based on the Compact PCI/PXI standard for fast data read-out to the host. It combines spectroscopy with waveform capture and on-line pulse shape analysis. The Pixie4 accepts signals from virtually any radiation detector. Incoming signals are digitised by 14-bit 75 MSPS ADCs. Waveforms of up to 13.6 μ s in length for each event can be stored in a FIFO. The waveforms are available for on-board pulse shape analysis, which can be customized by adding user functions to the core processing software. Wave-

forms, timestamps, and the results of the pulse shape analysis can be read out by the host system for further off-line processing. Pulse heights are calculated to 16-bit precision and can be binned into spectra with up to 32K channels. The Pixie4 supports coincidence spectroscopy and can recognize complex hit patterns.

Data readout rates through the Compact PCI/PXI backplane to the host computer can be over 100Mbytes/s. The PXI backplane is also used to distribute clocks and trigger signals between several Pixie4 modules for group operation. With a large variety of Compact PCI/PXI processor, controller or I/O modules being commercially available, complete data acquisition and processing systems can be built in a small form factor (more details on the Pixie system can be seen in the Appendix).” [9]

To process the data obtained by the Pixie system, the data that contains the raw pulse files can be replayed back through an open MCA program. This program allows you to measure certain aspects of a pulse. The pulse shape discrimination that was used in these experiments was to measure the rise times of the pulses between 10% and 90% of the pulse amplitude. The measured values are then stored along with the pulse amplitude at this measured rise time, figure 3.4 shows a picture of this idea, what these rise times are used for is further described in the upcoming experimental procedure section. By manually setting what range of rise times the pulses are likely to take along with the amount of data channels the program should assign to these values, the program can bin this data in accordance.

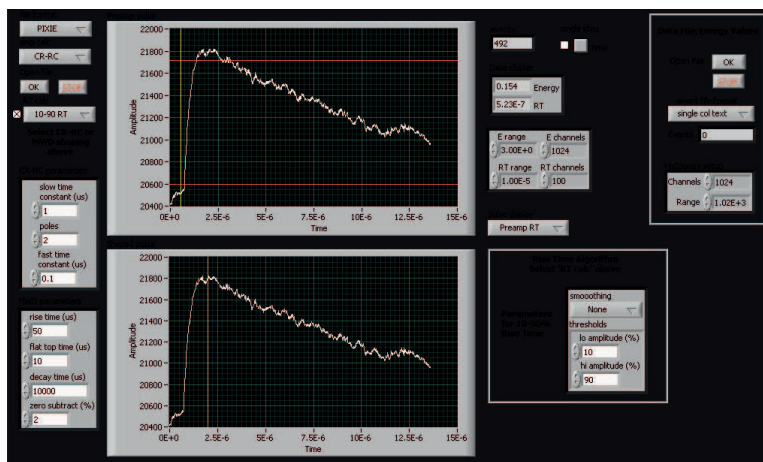


Figure 3.4: Rise Time Measurement for Pulse Shape Discrimination

3.2 Experimental Procedure

Gamma Source Experiments

For the initial run of gamma experiments where neutrons were not present, no digital pulse processing was needed, instead, traditional analogue pulse shaping methods were used. The gamma experiments were designed primarily to characterise the detectors as this had not been done before. A set of gamma sources, Cs, Co and a Na source were used. In each experiment one of the sources would be placed over the centre of the panel being tested, data acquisition would then commence for the same amount of time per source.

For the detector resolution the two Activated Perspex panels, which only differed by thickness were used. One of the Panels was 1" thick whilst the other was 1.5". Each panel was individually connected to a preamp then to a timing filter amp which had a constant integration time of 200ns and a constant differentiate time of 100ns set. The aim was to see how detector resolution varied around a Cs photo peak when the voltage to the photo-multiplier tube was itself varied. A range of 600 V to 950 V in steps of 50 Volts was tested, each time the voltage was changed the new spectrum was calibrated using a Na gamma ray source and then the Cs source itself. From

the results a detector resolution was identified along with a general statement on how well the panels could detect and tell the difference between gamma sources.

Collimated Gamma Source Experiments

With the initial gamma tests done, an experiment was carried out to see how parts of the panels reacted to a collimated Cs source. Each panel was placed above an automated motor system which can be controlled using software on a nearby computer. The motor system can move in both the X and Y planes and by making use of the software, move a minimum amount of 0.001 mm. The collimated source was mounted to the motor system and used to test the panels. Each panel was divided into a 5x5 grid; each section was 10 cm by 4cm and was scanned for a given time from the centre of each section before moving onto the next. After each scan the values needed (counts at Compton edge, FWHM and peak channel number) were obtained and recorded for use later, this was done manually by looking at the spectra obtained. The 1.5" panel had measurements taken for 300s a turn however the time for the 1" panel was doubled to 600s, as a longer time was needed to produce a clear result.

Once data had been collected for all sections of both panels, 3D mesh graphs were created in order to see clearly how the incident beam position changed the characteristics of the spectrum. Multiple readings were taken at each region and an average was calculated.

Gamma/Neutron Experiments

For the neutron experiments, the analogue pulse processing system was swapped out for the Pixie 4 system. When Slow neutrons were required one of the panels was placed over the neutron tank. This would therefore expose the panel to slow neutrons. For fast neutrons, a pipe filled with air can be moved between the panel and the source as to remove the water that causes neutron moderation, therefore creating a collimated fast neutron

beam.

The digital pulse processor that was used in these experiments was the Pixie4 system and was designed by a company called Xia who specialise in radiation detection methods and applications. For the system to work properly, a set of initial variables must be set, these relate to what form of pulses the system is looking for. The variables to set are mainly for the purpose of allowing the system to know when to trigger on the right sort of pulse. Settings include minimum pulse height to trigger on, the length in time in which it takes to reach this height and how long (including decay time) a pulse should be. To obtain a rough set of initial variables for the system, an oscilloscope was set up in conjunction with the detector to view the raw pulses entering the system and manual measurements were taken. Once these had been placed into the Pixie4 tests were run with the 1.5" Unactivated panel to better refine the values.

The experiments themselves involve placing the panels over the neutron tank with a Li sheet in place. A data acquisition is then recorded and stored in the system to be processed later. The tests have different parameters involved in order to produce data that can lead to the separation of gamma from neutron pulses.

Using an open MCA program written in lab view, the raw pulses were then processed so that conclusions could be drawn. The open MCA program is designed to record the rise times of all the input pulses against the energy they were representing and how many times they occurred. This was done with the use of a 2D graph representing 3D data. Figure 3.5 shows an example of this graph, the X axis represents the energy/amplitude of the pulse, the Y axis represents the rise time and the brightness of the pixel represents the occurrence. The brighter the pixel, the more counts for this pulse. This graph was set up from inside the program.

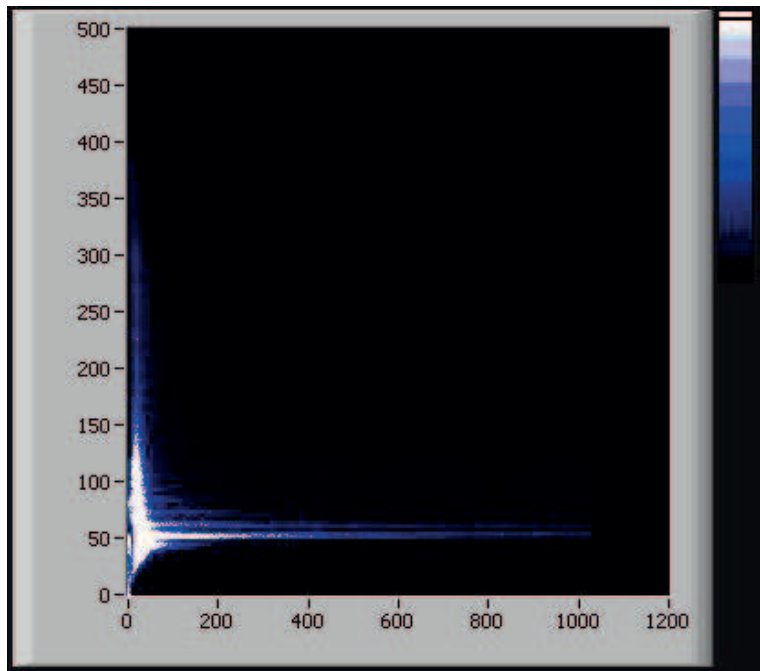


Figure 3.5: Example of the rise time Vs energy plot, the x axis represents the energy of the pulse whilst the y represents the associated rise time

This data can then be used to plot either an energy spectrum or a graph of rise times, using the rise time graph the pulses which have been created due to the neutron reactions with the Li, can be identified.

Chapter 4

Gamma Work

4.1 Detector Resolution Work

4.1.1 Detector Resolution

For clarification purposes, an Unactivated or Activated panel refers to the Plastic part of the detector. If it is Unactivated the panel is not gamma sensitive whilst an Activated panel is. If the Zn/S layer is present, the setup is now sensitive to neutrons. If cadmium is present the panel is still neutron sensitive, however it is now going to see less as the cadmium shields the panel from some of the neutrons but not all of them. The neutron source also emits a spread of gamma radiation.

Detector resolution is a measure of how good a detector is at differentiating between two energies that appear in a complex spectrum. In the simplest case it can be described as how well a detector can separate photo peaks and tell the energies of these peaks apart. The resolutions of Hyper Pure Germanium Detectors (HPGe) are usually very good and will produce large narrow peaks which are well defined and easily distinguishable when acquiring a spectrum by using equipment such as a Multi Channel Analysers (MCA). A Sodium Iodide detector will offer less resolution, so in the case where multiple energy peaks are present in a spectrum, some overlap between the peaks may be present. In a more complex spectrum the need for a higher resolution detector is therefore needed, usually a higher price.

To know if the provided scintillation panels were going to be good enough for the experiments, a value for their resolution was needed (see 2.6). After having run a couple of data acquisitions it was noted that there was no gamma photo peak present to take a FWHM measurement from, only a Compton continuum. This problem can occur in low Z materials, to acquire a value for the detector resolution; the max amplitude for the Compton Edge was found, this value was then divided in half. This value on the Compton edge was then found and the energy difference between the maximum amplitude and the new value was found and doubled. This final value is effectively the FWHM giving a detector resolution. This value may not be completely accurate but it does tell us if the panels are good enough and if found at different gain voltages, what voltage the detectors should be run at to give the best detector resolution.

4.1.2 Results

The following are the results obtained for the 1" Perspex panel.

1" Detector Panel Resolution

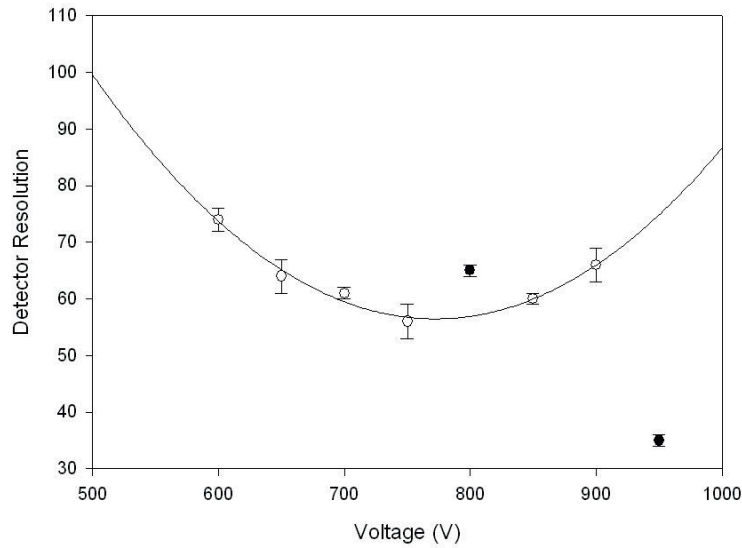


Figure 4.1: Detector Resolution for 1" Activated Panel No Neutrons Present

The best line fit was assumed to take the form of a quadratic equation $Y = Y_o + ax + bx^2$, using a computer program to calculate values for Y_o , a and b . The best detector resolution according to this fit was found to be around 760 V giving a resolution of about 55%. The black data points were omitted from the fitting calculations as they do not seem to fit the data.

The Following are the results obtained for the 1.5" panel.

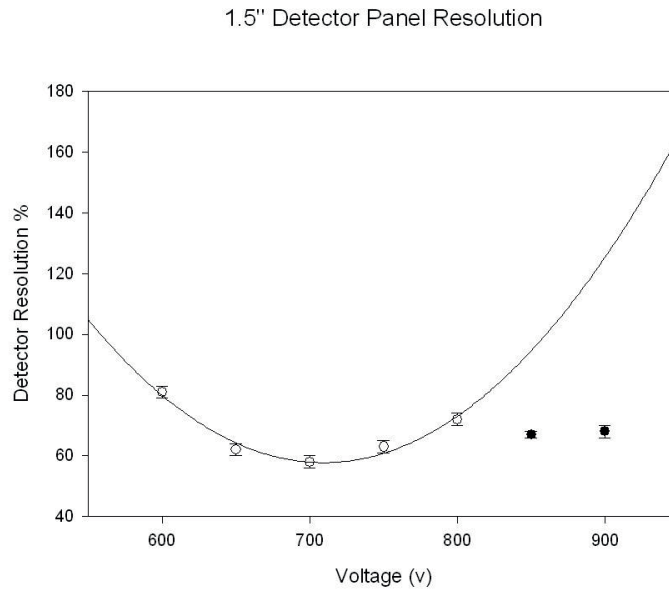


Figure 4.2: Detector Resolution for 1.5" Activated Panel No Neutrons Present

Best resolution around 720 V at about 56%.

As expected the low Z material scintillation panels have a low detector resolution, however the voltages that provide the best resolution are within a small range which is ideal. The data for voltages too high for the specific PMT in question became too noisy to analyse correctly, this results in bad data in the form of the black data points, as such these were ignored. From this it was decided that all future tests would have the panels running at 750 V as this would be one less variable to control and 750 V provides an acceptable resolution.

4.2 Collimated Cs Source Work

4.2.1 Collimated Cs Source

This experiment was designed to see how the characteristics of a spectrum changed, when a collimated gamma source was incident on to a specific region of the scintillation material, as apposed to allowing radiation to wash

over all areas of the panel as was done when performing the earlier gain and resolution work. Using an 800 MBq collimated ^{137}Cs source both the 1" and the 1.5" scintillation panels were scanned and measurements of where the peak Channel appeared were taken along with the counts at the peak and the Full Width Half Maxima at this point.

If the results obtained varied too much, then some serious thought would have to be given towards whether the panels would be suitable or not.

4.2.2 Results

As only two of the panels are sensitive to gamma rays, there are only two sets of results, one for the 1" Activated panel, and one for the 1.5" Activated panel. The following are 3D graphs that represent the position on the panel with the axis labeled Y, being the side of the panel that the PMT is connected to. This is true in all cases apart from the FWHM graph for the 1" Activated panel. the Z axis then represents the value for the measured variable at that point on the panel.

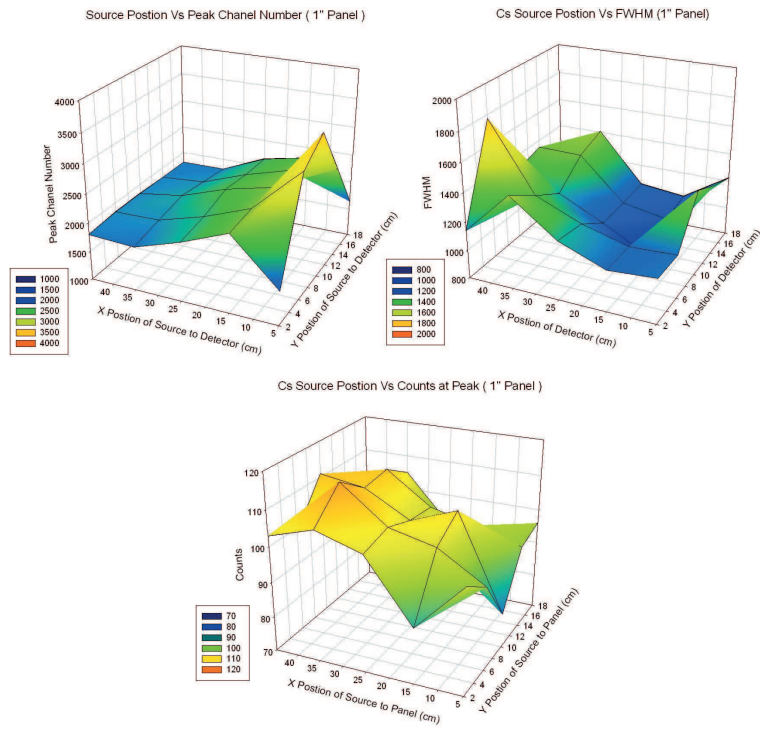


Figure 4.3: Collection of results for the 1" Activated Panel when exposed to a Cs source, No Neutrons Present

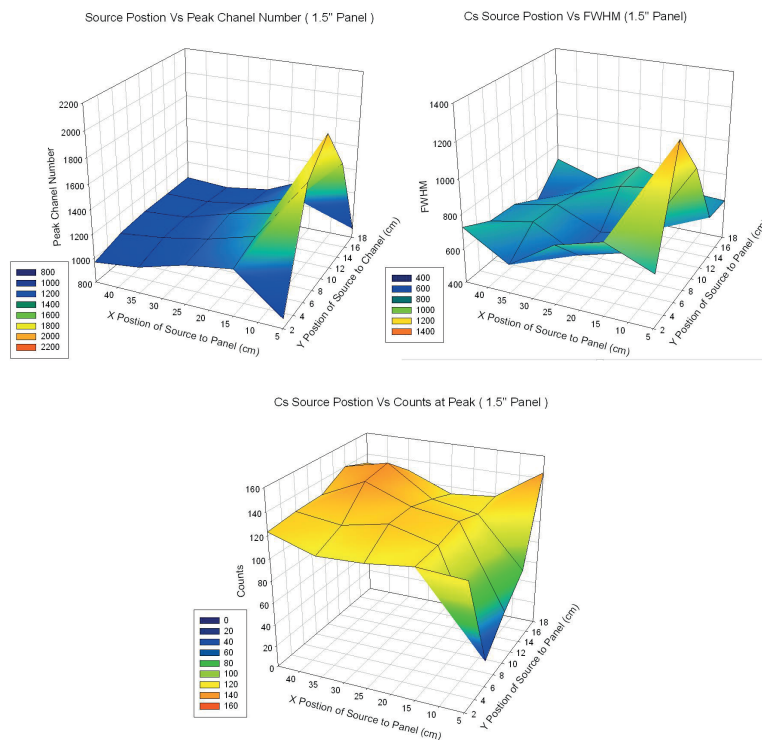


Figure 4.4: Collection of results for the 1.5” Activated Panel when exposed to a Cs source, No Neutrons Present

Peak Channel:

The data shows a clear pattern that is the same for both panels, as the proximity to the PMT increases, as does the channel number at which the peak energy appears. This is not surprising as the closer the origin of the light is to the PMT, the less likely it is to scatter before it enters the tube, this means more high energy beams will be detected than if the source of the light was further away or shielded from the PMT in some way. This idea is supported by the fact that the channel number for the peak drastically decreases in the corners closest to the PMT as most light will not be able to enter the PMT from here without first scattering at least once before. The pattern is symmetric down the centre.

FWHM:

For both panels the spread of the FWHM seems to be random suggesting that the main cause for the difference in these measurements is more likely due to the inability to measure this value to a high degree as I am using the Compton edge of the spectrum as the photo peak is missing. In both cases there is a case of a higher FWHM to the rest of the panel, this occurs at different regions in the two panels suggesting that either the result is odd or that there may be a manufacturing defect at this point.

Counts:

For both panels the spread of counts is roughly (excluding the results closest to the PMT for the 1.5" panel) the same over the whole panel which is to be expected however, as the 1" panel had 600s to accumulate data as apposed to the 300s that the 1.5" panel had it can be said that the 1.5" panel is a better detector as the amount of counts it sees is the same. The amount the FWHM and peak channel number changes in this panel is also smaller than that of the 1" panel.

The panels behave as expected however the change in channel number that was seen was higher than what I was hoping as it at least doubles when the source is moved from one end of the panel to the other, how this will affect neutron readings later when the whole panel is irradiated is yet to be seen.

4.3 Gamma Work Discussion

The conducted gamma radiation work shows that the design of the panels and the materials that they are made of, are good enough to be used as radiation detectors. For the tests that where conducted after this, in order to find a way to distinguish gamma rays from neutrons, the detector resolution work shows that all the panels can be run at the same voltage (750 V). If at some point these panels were set up like the Rad-Nuke portal discussed in

the introduction, to produce one spectrum from several panels, they would have to be gain matched as the channel numbers that energy peaks appear at would be different. However this is not needed for the following neutron work as only data from one panel at a time is analysed.

The collimated Cs source work shows that the panels behave and show similar characteristics when exposed to the same type of radiation, this is good as it means comparisons can be drawn between the two. The results show the 1.5" Activated panel detect more events than the 1" Activated panel in the same time, is interesting but does not affect the future work. In future it should be seen if it is the added thickness of the panel that results in the greater amount of counts.

Chapter 5

Neutron Work

5.1 Oscilloscope Trace Work

5.1.1 Oscilloscope Traces

After having run many tests using the two activated panels for gamma rays, using a neutron source and separating out the pulses due to neutrons and gammas was the next step. To understand how to correctly do this, an oscilloscope was used to look at and record the raw pulses coming from the panels before the signals are digitised. By looking at the pulses on the scope, one will be able to clearly see what a neutron, gamma and noise pulse looks like before it actually enters the Pixie4 system. From the first few tests it was seen that a preamp was needed to be used between the panel and the Pixie4 system as without it the signal gets reflected due to an impedance difference, creating a multitude of reflected pulses, however with the amp there is a risk that any sort of rise time difference between pulses is being destroyed by the integration process of the amp as it is not fast enough. Along with telling pulses apart the oscilloscope is needed to see if the preamp destroys the rise time difference too much to be useful.

For these tests the 1.5" Activated Panel and the 1" Unactivated Panel were used, as one panel that could see gamma and neutrons and one that could see only neutrons were needed so results could be compared. For each panel, the pulses being produced when the panel was over the tank, over the tank

with cadmium and away from the tank were observed. For test a pre amp was used and then again without.

5.1.2 Oscilloscope Results

1" Unactivated panel

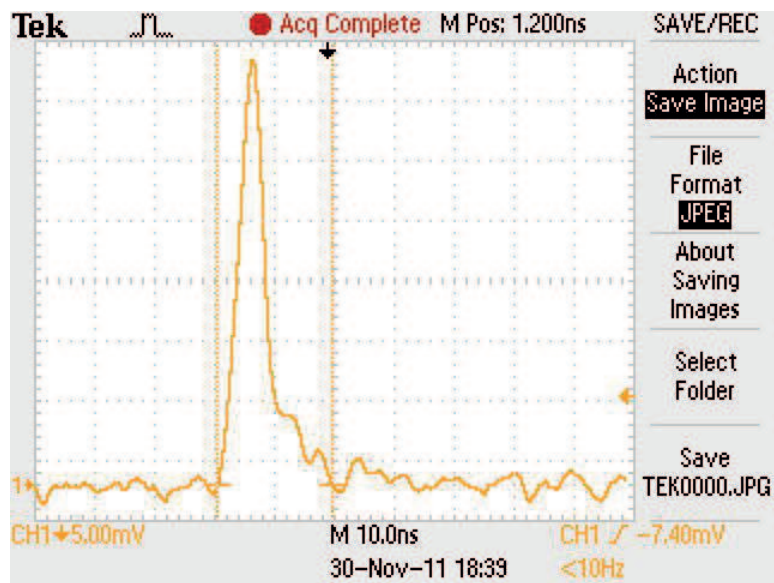


Figure 5.1: The oscilloscope trace as seen on the screen for the 1" Unactivated Panel with no pre amp over the neutron tank, pulse width = 20 ns

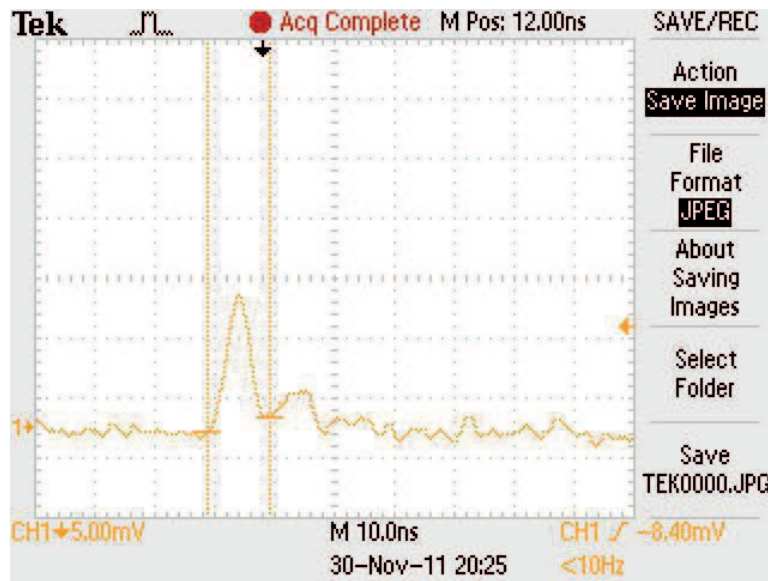


Figure 5.2: The oscilloscope trace as seen on the screen for the 1" Unactivated Panel with no pre amp away from the neutron tank, pulse width = 10 ns

By just looking at the first two traces, it can be seen that the pulses seen do vary when the panel is over and away from the tank. Not only are the amplitudes of the pulses less when the panel is away from the tank, but so are the pulse widths. By adding a pre amp into the system the pulses are integrated and take the following form. In the case where a preamp is not present, there is a second smaller bump following the first. This is probably an oscillation due to ringing or reflection of the signal. This problem arises when a cable with badly matched impedance to the Pixie4 system is used, by integrating the signal with a preamp, this problem is removed.

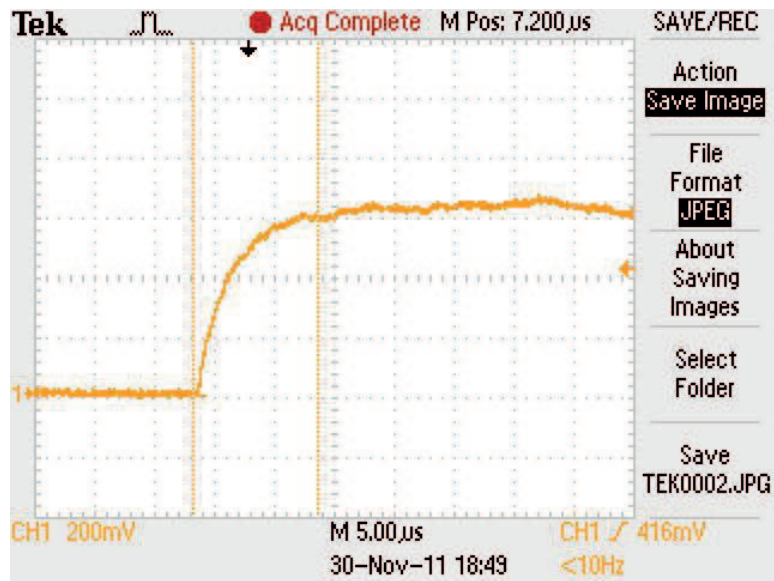


Figure 5.3: The oscilloscope trace as seen on the screen for the 1" Unactivated Panel with a pre amp over the neutron tank, rise time = $10.4 \mu s$

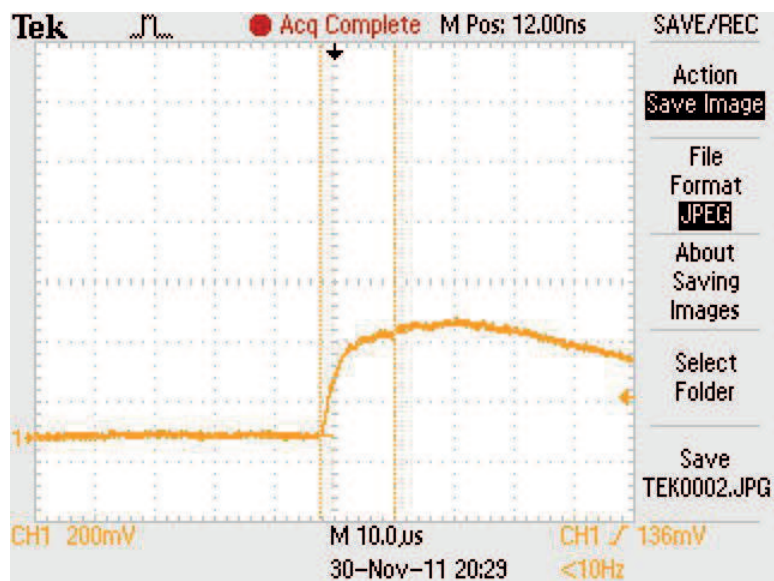


Figure 5.4: The oscilloscope trace as seen on the screen for the 1" Unactivated Panel with a pre amp away from the neutron tank, rise time $12.4 \mu s$

At first, the results look worrying as the rise times appear similar however it should be noted that the count rate for the pulses away from the tank is notably less than when the panel is over the tank. A second thing to note is the amplitude of the pulses. Those relating to when the panel is away from the tank, have a much lower amplitude relating to a lower energy pulse. Later discrimination work should therefore be able to be able to separate these noise pulses from the neutron ones. As a preamp will be used no more signal samples without an amp will be shown. It is important to note that the pulse widths of all the non integrated signals are in the order of 10 ns whilst the integrated ones are in the order of 10 μ s.

1.5" Activated Panel

The pulses produced when using the gamma sensitive panel, are noticeably faster which is expected from the theory as gamma pulses should be, this looks hopeful for future work however as the amount of gamma pulses seen is so high it was difficult to obtain a pulse that resembled the neutron pulses as seen in the Zn/S scintillator as seen in the 1" Unactivated panel. How this will effect the overall result is yet to be seen, if the amount of pulses the system can see a second, is too small the gamma pulses could drown out the neutron pulses in the Activated panels.

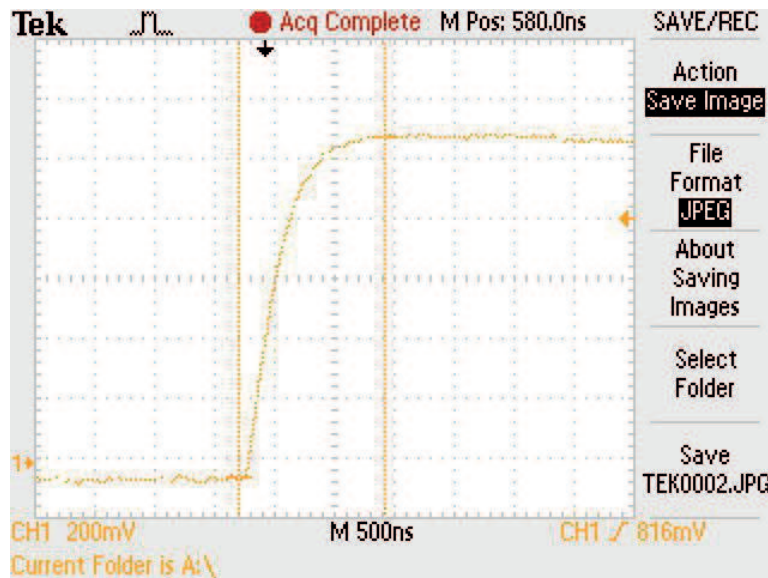


Figure 5.5: The oscilloscope trace as seen on the screen for the 1.5” Unactivated Panel with a pre amp over the neutron tank, rise time = $1 \mu\text{s}$

5.2 Rise Time Measurement and Zn/s Gamma Sensitivity

5.2.1 Rise Times

After having seen that the rise times being produced in the Zn/S layer are notably longer than the gamma pulses in the plastic layer, why is it so hard to separate the two? Something that must be looked into before any theories can be investigated, is that it must be confirmed just how sensitive the Zn/S layer is to gamma rays. To investigate this, the 1” Unactivated panel has had four sets of experiments done on it using the Pixie4 system to record the raw pulses. In all four experiments, the Zn/S layer doped with Li is present, in the first two tests the panel is exposed to the neutron source with and without the cadmium present. In the second two tests the panel is away from the neutron source and exposed to a Cs gamma source and then to no source. By looking at these four sets of data fully processed, one should be able to say if the Zn/S layer is gamma sensitive and if so, is it a problem (see the experimental procedure 3.2 to see how this was done).

The following are the results for the 1" Unactivated panel, as a contol the first set of figures, are for when there is no radiation source present.

1" No Source

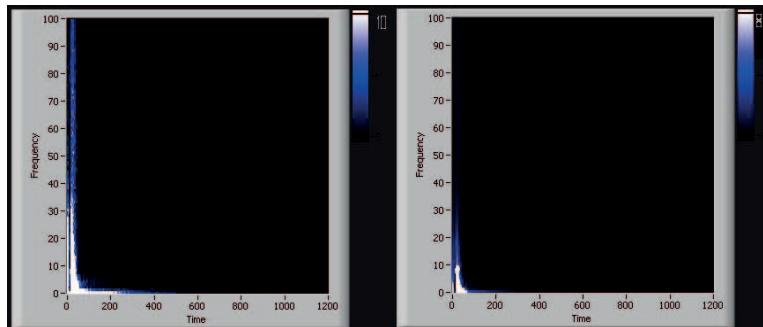


Figure 5.6: 2D plots of the pulses seen when the 1" inch unactivated panel is not exposed to a source

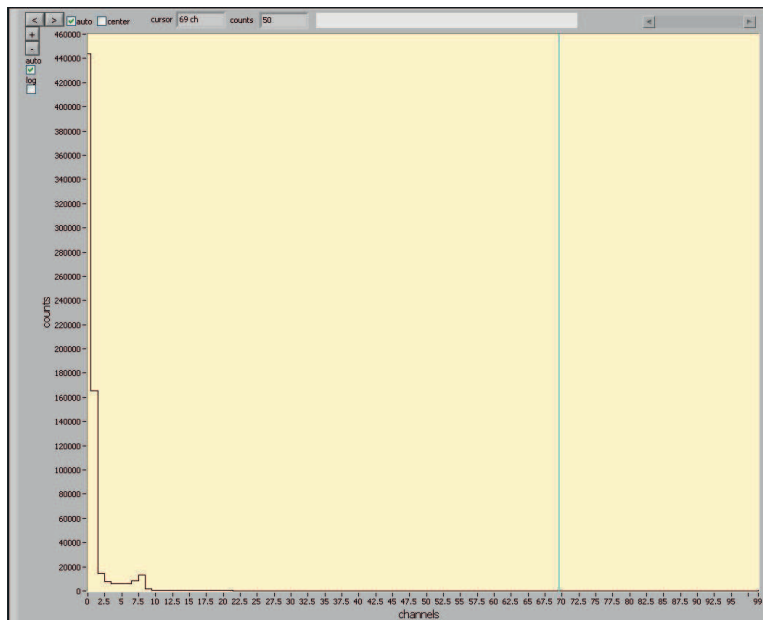


Figure 5.7: Rise Time plot of the pulses seen when the 1" inch unactivated panel is not exposed to a source

Manually setting the value for how many counts a white pixel represents allows you to analyse the figures better. As such all the 2d plots on the left have the white pixels set to 10 so all events can be seen. The plots to the right represent when all the noise/weak pulses disappear and only the strongest pulses are present. The value that this occurs at can be seen to the top right of the figures. For the no source results it can be seen that not many pulses are seen at higher rise times but there is a big noise peak due to electrical noise in the first couple of channels. The slightly smaller peak at channel number 8 could be a feature and this should become clear after more results.

1" Neutron Results

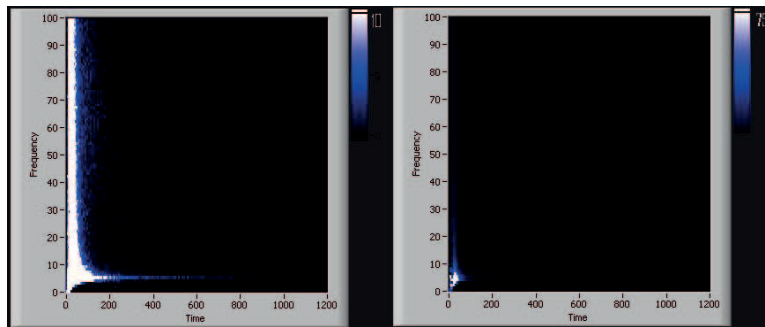


Figure 5.8: 2D plots of the pulses seen when the 1" inch unactivated panel is exposed to the neutron source with the Zn/S layer present

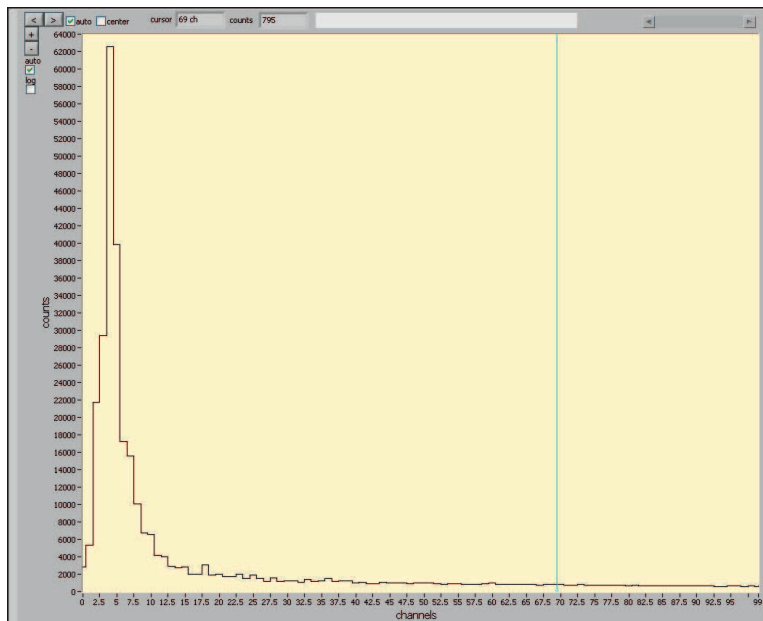


Figure 5.9: Rise Time plots of the pulses seen when the 1” inch unactivated panel is exposed to the neutron source with the Zn/S layer present

1” Neutron Results with Cadmium

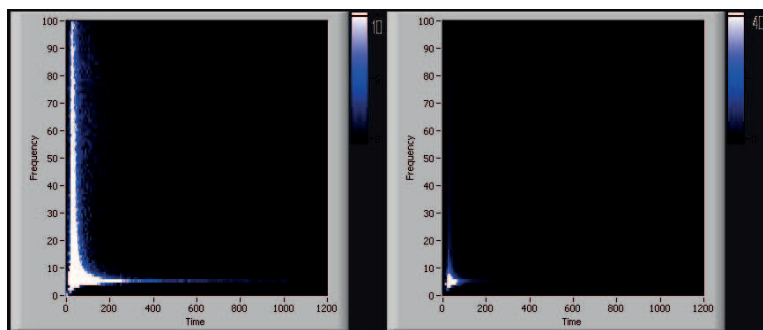


Figure 5.10: 2D plots of the pulses seen when the 1” inch unactivated panel is exposed to the neutron source with the Zn/S layer present and wrapped in Cadmium

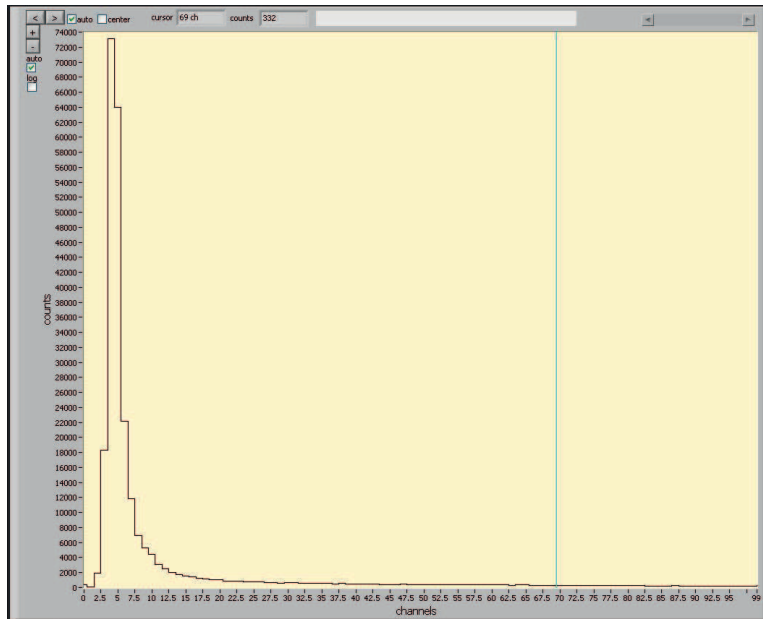


Figure 5.11: Rise Time plots of the pulses seen when the 1" inch unactivated panel is exposed to the neutron source with the Zn/S layer present and wrapped in Cadmium

Looking at the two 2D plots for the neutron source, it looks like neutrons are being seen at the higher rise times, however the cadmium is not stopping all of the neutrons. This can be seen in the fact that both graphs have the bump in the higher rise time regions of the 2D plots, however it is more intense in the 2D plot relating to the experiment where the cadmium is not present. This feature is only present when neutrons are present, which would suggest the two are linked.

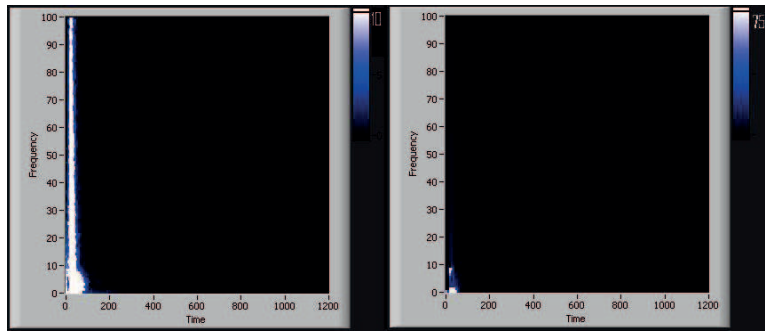


Figure 5.12: 2D plots of the pulses seen when the 1” inch unactivated panel is exposed to a Cs source

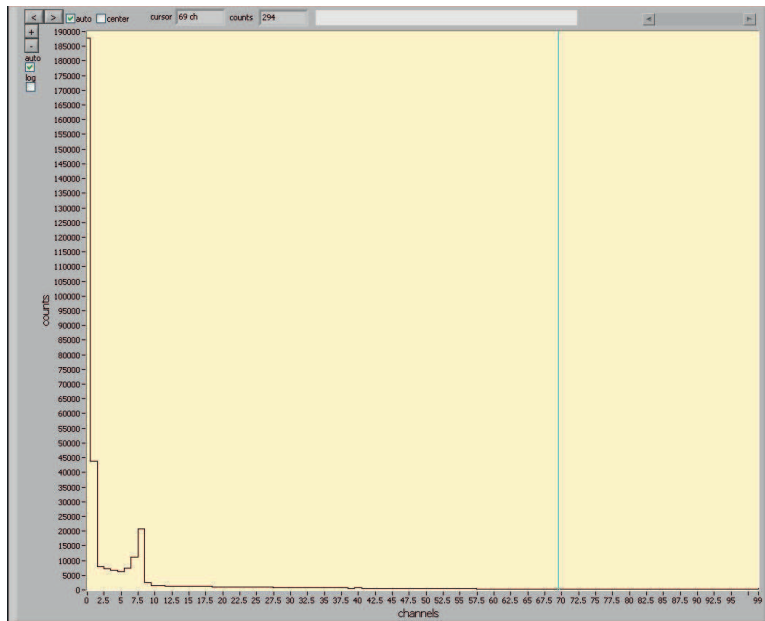


Figure 5.13: Rise Time plot of the pulses seen when the 1” inch unactivated panel is exposed to a Cs source

From looking at the Cs results there appears to be more events in the higher rise time regions as well as in the second peak. It can be said already that the pulses linked to noise appear in the first few channels only as this feature appears in all of the results so can be ignored when analysing. As the second peak has grown as well as the amount in the higher rise time regions it looks like Zn/S is gamma sensitive, if however the majority of the gamma

pulses appear in the second peak as apposed to the higher rise time regions then this is not a problem. Another aspect that can be looked at is how an activated panel without the Zn/S reacts to the Cs source. By comparing the ratio of counts in the second peak to the higher rise time section conclusions can be made.

1.5” Activated Cs Results

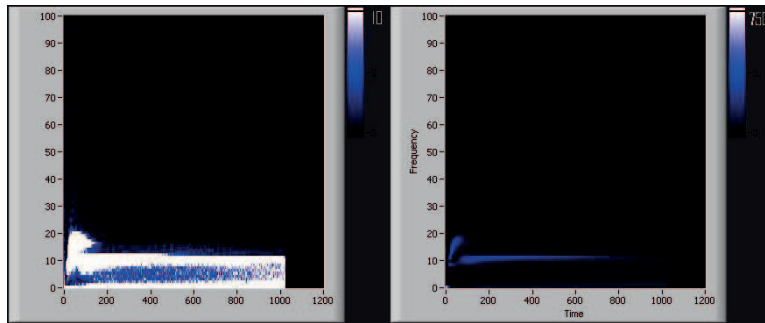


Figure 5.14: 2D plots of the pulses seen when the 15” inch activated panel is exposed to a Cs with the Zn/S layer present

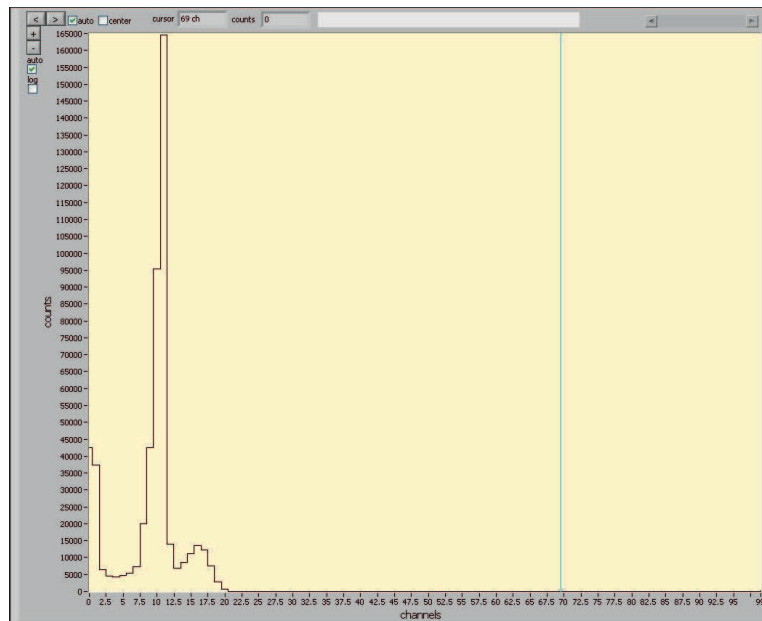


Figure 5.15: Rise Time plot of the pulses seen when the 15” inch activated panel is exposed to a Cs with the Zn/S layer present

A new feature appears which is expected since the activated panel is adding a new set of gamma results to the spectrum, this too will have it's ratios compared. If it is found that there are gammas at higher rise times, this will not be a problem as it will just mean that along with measuring rise times to discriminate, pulse height analysis will also be used to omit long rise time, low energy pulses from the neutron part as these will most likely be gammas.

5.2.2 Ratio Results

To compare ratios the rise time spectra were divided into 2 sections as can be seen in figure 5.16. N1 corresponds to the peak that seems to grow when gammas are present and N2 represents the region where the neutron events fall along with some gammas. If the ratio of counts in N1 is higher than the counts in N2 when Cs is present when compared to the ratio of N1 to N2 when the panels are over the neutron tank, less pulse discrimination will be needed later to separate the gammas from the neutrons at least in the Unactivated panels.

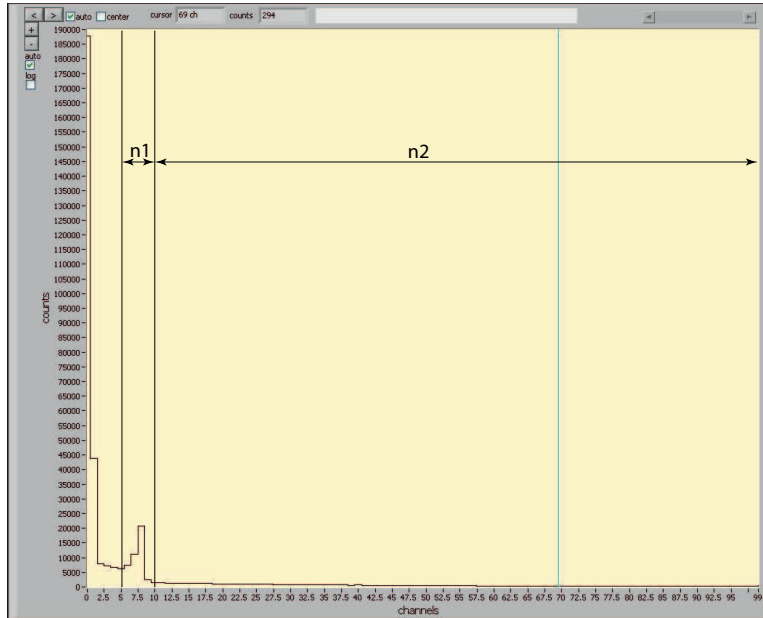


Figure 5.16: Example of the ratio regions in the Rise Time spectra

The following is a table of the ratio results with the conditions the panel was in and what it was exposed to. Li means over the neutron tank with no cadmium, Cad means over the tank with a sheet of cadmium, Cs means away from the tank but with a Cs source present and No source means away from the tank and no source.

Panel	Condition	n1:n2
1" Unactivated Zn/S	li	1:0.517
	Cad	1:0.259
	Cs	1:0.752
	No Source	1:0.243
1.5" Activated No Zn/S	Cs	1:0.220
1.5" Activated Zn/S	Cs	1:0.100

The results for the 1" panel are good as it shows that more counts are present in the higher rise time reasons when the neutron sensitive version of this panel is exposed to the neutron source. However the fact that the ratio

for the Cs source is higher shows that not only is the Zn/S gamma sensitive, but that the pulses produced fall within the higher rise time regions. The results for the 1.5" Activated panel show however that a lot of the events due to gammas are added to the first peak as the ration of N1 to N2 decreases when the Zn/S is present.

5.3 Pulse Shape Discrimination

5.3.1 Conditions used for seperation

Having done the preliminary work it can be seen that in the Unactivated rise time spectra, there is a clear area where one can say the events are purely coming from pulses related to neutron pulses emanating from the Zn/S layer. By making use of some of the properties of the open MCA program one can import the raw data into a spreadsheet and then manipulate it. By gating off the higher rise time regions energy spectra can be created where the counts due to neutrons can be manually moved further up the energy axis of the spectra so that the correct energy distribution of events can be shown (see the detector design section for details on why this is needed).

The following is the created energy spectrum that has been made from the raw data relating to the 1.5" Unactivated panel, when it joined to the Zn/S layer and placed over the tank.

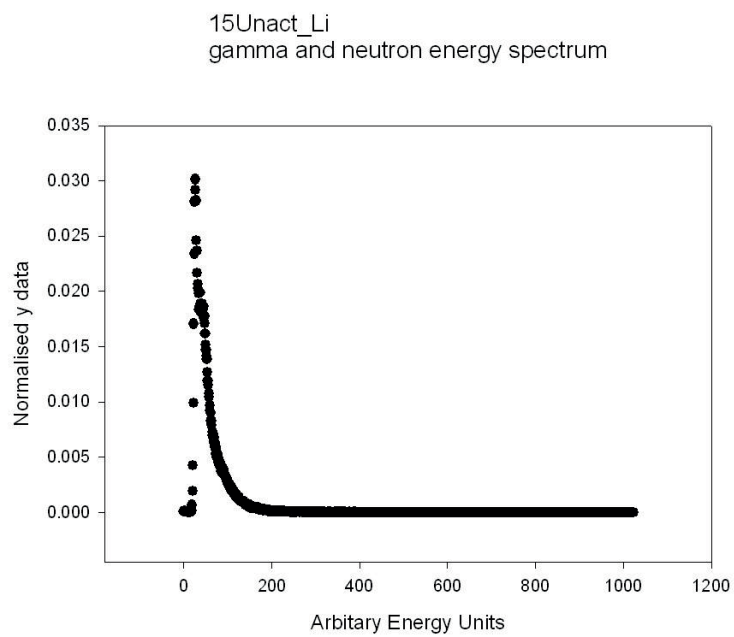


Figure 5.17: Normalised Energy Spectrum for 1.5” Unactivated Panel, Neutrons present

By now taking out all of the counts from the first peak that have rise times of 20 arbitrary units or more (neutron pulses), this spectrum can be corrected.

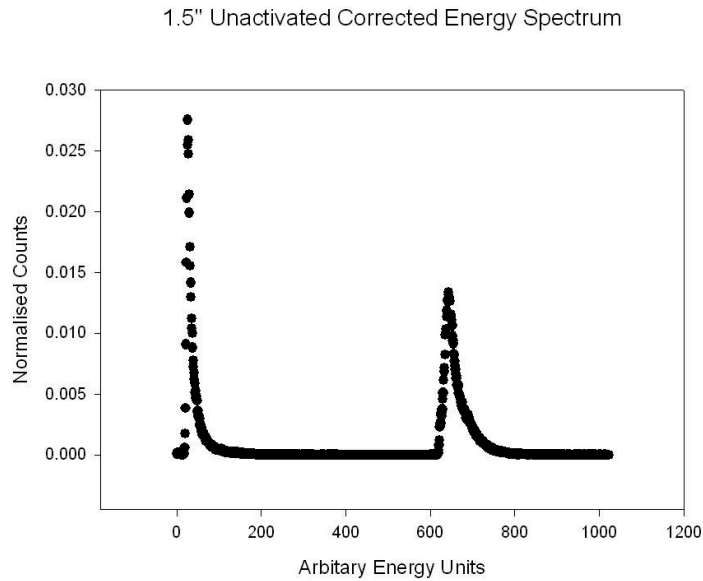


Figure 5.18: Normalised Corrected Energy Spectrum for 1.5” Unactivated Panel, Neutrons present

This looks good because looking at the uncorrected spectrum a bump in the main peak can be seen at channel number 150 that peaks at a normalised count amount of 0.018. This bump is not present in the corrected one (figure 5.18). It is my opinion that this bump is the neutron peak that has now been repositioned. The reason the peak is no longer quite as high (It now peaks at 0.015) is because there would be some shorter pulses with higher energy that were previously mixed in but have now been filtered out.

Unfortunately as it stands at the moment, this can only be done for the Unactivated panels as the neutron events are not showing up in the activated panels strongly enough if at all. There are a number of reasons that could be the cause for this, but the main reason is probably that due to the fact that the gamma rays that are also coming from the source are so strong, tied in with the fact that the equipment itself can only see a percentage of the events and not all of them, it seems the gamma events are drowning out the neutron ones this can be seen when you compare the rise time spectra of the 1.5” Activated and Unactivated panels when focused in on the higher

rise time regions.

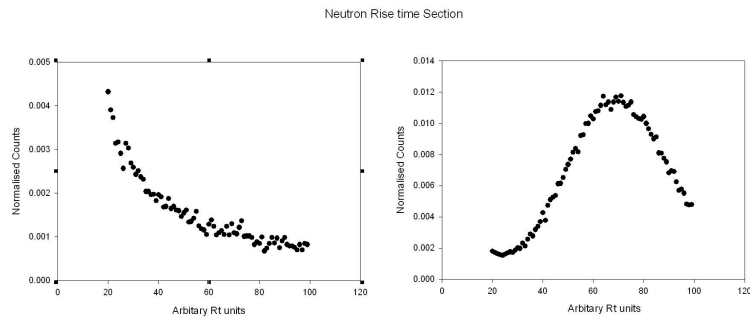


Figure 5.19: Comparison of the form the rise time spectra take at higher rise times.

It can be seen that in the right graph representing the 1.5 Unactivated panels there is a clear feature that can be gated whilst in the left 1.5 activated graph there is no feature and just a spread instead. It is beginning to look like separating out gammas from neutrons in the Activated Panels is not possible as there is just no clear feature of the rise time graphs that can be said are neutron only events. For the Unactivated panels however the rise time graphs do show neutron only features that are not in the rise time spectra for the same panels when the neutrons are removed. Separating neutrons from noise is possible however gammas from noise from neutrons will require more work.

Chapter 6

Conclusions

By using more advanced digital pulse processing then traditional analogue circuitry, it has been shown that a lot more data can be measured from a signal pulse other then just its amplitude. Pulses have succesfully had their rise times measured and plotted against thier energies along with how many times similair pulses occurred.

Although the goal, of being able to separate neutron events from gamma events by only taking one set of readings from a source has not been successful, the results show promise. First ignoring any of the reasons related to the DPP that may be the cause for this failure, separating out neutrons from noise and gammas within the Zn/S layer has had some success. The rise time spectra relating to the Unactivated panels, show a clear feature that is not present when the neutron source is taken away. This therefore is undoubtedly the area in the rise time spectra relating to the neutrons. This feature however is not present within the Activated panels. After analysing all of the data and comparing the two types of panel and how they react when exposed to the same set of conditions, a reason for why this is, has been deduced.

It seems that as the Zn/S layer and the Activated panels are gamma sensitive, any spectra, be it rise time or energy, produced when the two materials are combined, have to many gamma events and not enough neutron events.

The Pixie4 may be missing some of the pulses that the PMT produces and because there are a significant amount more gamma events to neutrons only a few neutron events may be recorded. This means that any feature the neutron events are adding to the rise time spectra for the Activated panels, is dwarfed by the features that the gamma events are adding.

In future the 1.5" panels should have work done on them to better understand the effect the neutron sensitive layer has on them. By taking a run of data when the panel is exposed to the tank without the Zn/S layer and then again with a simple data subtraction can be done to produce a rise time spectrum of only the Zn/S layer. If this spectrum is then compared to the results of the Unactivated panels with the Zn/S layer and neutron source, and found to be similar, the neutrons can be separated out within Activated panels. However if this is done and still no feature is present, it means one of two things, either that a "faster" system is needed or the Activated plastic layer is too sensitive to gammas and may need to be replaced with one that is not.

It would seem that this work is interesting and needs more work done on it to understand just how far one can take digital pulse processing. If successful cheaper more efficient detectors could be made that perform better fulfilling what Rapiscan want.

Chapter 7

Acknowledgments

The author would like to thank Professor Paul Sellin and Dr Annika Lohstroh for all the support and guidance given throughout this project. The author would also like to thank Dr Ed Morton from Rapiscan for providing the project and materials needed to conduct it. Thanks would like to be given to all the other students in the department who were always willing to help when it was needed. Final thanks is given to Glenn F. Knoll for writing easily the best book on radiation detection that covered all the needed theory to carry out this project.

Bibliography

- [1] B.R. Martin: **Nuclear and Particle Physics**, 2nd Edition, Wiley, 2009, 1-2, 62-63
- [2] P. Rinard: **Neutron Interactions With Matter**, 1991
- [3] Nucleus decay: http://en.wikipedia.org/wiki/File:Gamma_Decay.svg, Accessed on 10/01/2012
- [4] F. Knoll: **Radiation Detection and Measurement**, 4th edition, Wiley, 2010, 519-553, 224-233, 235-257
- [5] W.N. Cottingham, D.A. Greenwood: **An Introduction to Nuclear Physics**, 2nd Edition, Cambridge, 2001, 199-213
- [6] University of Surrey, RDI Lab Script: **Neutron Spectroscopy with Organic Scintillators**, 2009
- [7] Compton Scattering: http://missionscience.nasa.gov/ems/12_gammarays.html, Accessed on 10/01/2012
- [8] Compton Continuum: <http://en.wikipedia.org/wiki/File:Am-Be-SourceSpectrum.jpg>, Accessed on 12/01/2012
- [9] Pixie4 User Manual: **User's Manual Digital Gamma Finder (DGF) Pixie-4**, Version 2.40, XIA LLC
- [10] Dr W. Gilboy (University of Surrey): **RDI Lecture: Neutron Detection & Instrumentation**, 2012
- [11] B.I. Stepanov, V.P. Gribkovskii: **Theory of Luminescence**, Iliffe Books Ltd, 1968, preface and chapter 1

- [12] Scintillation Detector: <http://en.wikipedia.org/wiki/File:Photomultiertube.svg>,
Accessed on 11/01/2012
- [13] Energy States Within a Molecule:
[http://chemwiki.ucdavis.edu/physical_chemistry/spectroscopy/
electronic_spectroscopy/electronic_spectroscopy%3a_theory](http://chemwiki.ucdavis.edu/physical_chemistry/spectroscopy/electronic_spectroscopy/electronic_spectroscopy%3a_theory),
Accessed on 18/01/2012
- [14] R.L. Craun, D.L. Smith: **Nuclear Instrumentation Methods**,
1970
- [15] University of Surrey, RDI Lab Script: **RDI21: Digital DAQ and
Gamma Ray Spectroscopy**, 2011
- [16] N. Calvert: **RadNuke Neutron Detection Efcieny**, 2011

Appendix

All the work here comes directly from [9]

Features

- Designed for high precision gamma-ray spectroscopy with HPGe detectors.
- Directly compatible with Scintillator/PMT combinations: NaI, CsI, BGO, and many others.
- Simultaneous amplitude measurement and pulse shape analysis for each channel.
- Input signal decay time: as fast as 150ns and up to 10ms, exponentially decaying.
- Wide range of filter rise times: from 53ns to 109 μ s, equivalent to 27ns to 50 μ s shaping times.
- Programmable gain and input offset.
- Excellent pileup inspection: double pulse resolution of 50 ns. Programmable pileup inspection criteria include trigger filter parameters, threshold, and rejection criteria.
- Digital oscilloscope and FFT for health-of-system analysis.
- Triggered synchronous waveform acquisition across channels, modules and crates.
- Dead times as low as 1 μ s per event are achievable (limited by DSP algorithm complexity). Events at even shorter time intervals can be extracted via off-line ADC waveform analysis.
- Digital constant fraction algorithm measures event arrival times down to a few ns accuracy.
- Supports 32-bit 33 MHz PCI data transfers (\approx 100 Mbytes/second).

Specifications

Front Panel I/O	
Signal Input (4x)	4 analog inputs. Selectable input impedance: 50 Ω and 5k Ω , \pm 5V pulsed, \pm 2V DC. Selectable input attenuation 1:7.5 and 1:1 for 50 Ω setting.
Logic Input/Output	General Purpose I/O connected to programmable logic (Rev. C, D only). Currently can be either used as input for global backplane signals <u>Veto</u> or <u>Status</u> , as an input for module specific logic level reported in the data stream, or as an external trigger.
Logic Output	General Purpose output from Digital Signal Processor. Function to be determined.
Backplane I/O	
Clock Input/Output	Distributed 37.5 MHz clock on PXI backplane.
Triggers	Two wired-or trigger buses on PXI backplane. One for synchronous waveform acquisition, one for event triggers.
Status	Global logic level from backplane reported for each event
Token	Global logic level from backplane used for coincidence tests
Synch	Wired-or SYNC signal distributed through PXI backplane to synchronize timers and run start/stop to 50ns.
Veto	Global logic level to suppress event triggering.
Channel Gate	Individual GATE to suppress event triggering for each channel with use of PXI-PDM (Rev. D only)
Digital Controls	
Gain	Analog switched gain from 0.97 to 11.25 in max. 10% steps. Digital gain adjustment of up to \pm 10% in 15ppm steps.
Offset	DC offset adjustment from -2.5V to +2.5V, in 65535 steps.
Shaping	Digital trapezoidal filter. Rise time and flat top set independently: 53ns – 109 μ s in small steps.
Trigger	Digital trapezoidal trigger filter with adjustable threshold. Rise time and flat top set independently from 26ns to 853ns.
Data Outputs	
Spectrum	1024-32768 channels, 32 bit deep (4.2 billion counts/bin). Additional memory for sum spectrum for clover detectors.
Statistics	Real time, live time, filter and gate dead time, input and throughput counts.
Event data	Pulse height (energy), timestamps, pulse shape analysis results, waveform data and ancillary data like hit patterns.

Figure 7.1: Tabel of Pixie4 Specifications